Methane from UV-irradiated carbonaceous chondrites under simulated Martian conditions

Andrew C. Schuerger,[1] John E. Moores,[2] Christian A. Clausen,[3] Nadine G. Barlow,[4] and Daniel T. Britt[5]

[1] A UV photolytic process was studied for the production of methane from carbonaceous chondrites under simulated Martian conditions. Methane evolution rates from carbonaceous chondrites were found to be positively correlated to temperature (-80 to $20°C$) and the concentration of carbon in the chondrites (0.2 to 1.69 wt%); and decreased over time with Murchison samples exposed to Martian conditions. The amount of evolved methane (EM) per unit of UV energy was 7.9×10^{-13} mol J^{-1} for UV irradiation of Murchison (1.69 wt%) samples tested under Martian conditions (6.9 mbar and $20°C$). Using a previously described Mars UV model (Moores et al., 2007), and the EM given above, an annual interplanetary dust particle (IDP) accreted mass of 2.4×10^5 kg carbon per year yields methane abundances between 2.2 to 11 ppbv for model scenarios in which 20 to 100% of the accreted carbon is converted to methane, respectively. The UV/CH_4 model for accreted IDPs can explain a portion of the globally averaged methane abundance on Mars, but cannot easily explain seasonal, temporal, diurnal, or plume fluctuations of methane. Several impact processes were modeled to determine if periodic emplacement of organics from carbonaceous bolides could be invoked to explain the occurrence of methane plumes produced by the UV/CH_4 process. Modeling of surface impacts of high-density bolides, single airbursts of low-density bolides, and multiple airbursts of a cascading breakup of a low-density rubble-pile comet were all unable to reproduce a methane plume of 45 ppbv, as reported by Mumma et al. (2009).

1. Introduction

[2] Methane (CH_4) has recently been detected in the Martian atmosphere at a global mixing ratio of 10–15 ppbv with spatial and temporal variations ranging between 0 and 45 ppbv [*Fonti and Marzo*, 2010; *Formisano et al.*, 2004; *Geminale et al.*, 2008, 2011; *Krasnopolsky et al.*, 2004; *Mumma et al.*, 2009]. Furthermore, spatially constrained methane plumes between 45 and 60 ppbv have been observed but appear to only persist for a few months [*Fonti*

[1]Department of Plant Pathology, University of Florida, Space Life Sciences Laboratory, Kennedy Space Center, Florida, USA.
[2]Department of Physics and Astronomy, Centre for Planetary Science and Exploration, University of Western Ontario, London, Ontario, Canada.
[3]Department of Chemistry, University of Central Florida, Orlando, Florida, USA.
[4]Department of Physics and Astronomy, Northern Arizona University, Flagstaff, Arizona, USA.
[5]Department of Physics, University of Central Florida, Orlando, Florida, USA.

Corresponding author: A. C. Schuerger, Department of Plant Pathology, University of Florida, Bldg. M6-1025, Space Life Sciences Laboratory, Kennedy Space Center, FL 32899, USA. (schuerg@ufl.edu)

and Marzo, 2010; *Mumma et al.*, 2009]. In contrast, others have argued that spatial and temporal heterogeneity of methane in the Martian atmosphere cannot be explained by known photochemical processes because the only currently accepted methane sink on Mars is a Lyman-α ultraviolet (UV; 121 nm) photolytic process in the upper atmosphere. The Lyman-α process suggests methane lifetimes on Mars of 250–670 years, and predicts that atmospheric mixing would quickly yield a uniform methane abundance in the atmosphere [*Lefèvre and Forget*, 2009]. There is currently acute interest in confirming the methane abundance on Mars because terrestrial methane (1.8 ppmv) is produced primarily from biological processes [*Keppler et al.*, 2006; *Quay et al.*, 1999], leading to the hypothesis that Martian methane might be an indication of a subsurface methanogenic microbial community [*Atreya et al.*, 2007; *Krasnopolsky et al.*, 2004].

[3] Reviews of recent literature [*Schuerger et al.*, 2011; *Shkrob et al.*, 2010] suggest that at least eight possible mechanisms may be involved in the production of CH_4 on Mars including (not in priority): (1) outgassing from comet and asteroid impacts, (2) outgassing from interplanetary dust particles (IDPs), (3) subsurface clathrates, (4) subsurface serpentinization of olivine, (5) UV photolysis of H_2O in the presence of CO yielding intermediates that can quickly

recombine to form methane, (6) geothermal outgassing, (7) presumptive biological processes, and (8) UV photolysis of organics. Of these mechanisms, the UV photolytic process for the formation of methane on Mars (henceforth, the UV/CH$_4$ model) has been confirmed recently for organic carbon, but not inorganic carbon, under simulated Martian conditions [*Schuerger et al.*, 2011] and will be the primary mechanism studied here.

[4] The most commonly accepted sources of organics on Mars are isotropically accreted interplanetary dust particles (IDPs; 90%) and low-mass carbonaceous chondrites (10%) [*Atreya et al.*, 2007; *Bland and Smith*, 2000; *Flynn*, 1996; *Flynn and McKay*, 1990]. *Flynn* [1996] estimates that IDPs in general contain ~10 wt% organics, and as much as 2.4 × 10^5 kg/yr of unaltered carbon (C) might be accreting to Mars. Thus, Martian regolith should contain between 0.2 and 2.9 wt% organic C (depending on model assumptions; and a 10 wt% C in IDPs) [*Flynn and McKay*, 1990]. But the Viking GCMS experiment failed to detect organics on Mars down to the ppm level [*Biemann and Lavoi*, 1979; *Navarro-González et al.*, 2010]. The paradox of not detecting what should be there has led to the proposal of diverse mechanisms that could degrade the meteoritic organic compounds on Mars. Of the various hypotheses that have been proposed to explain this paradox, the UV-mediated degradation of organics is the most favored [*Zent and McKay*, 1994; *Yen et al.*, 2000]. Furthermore, UV irradiation may act by three separate processes to degrade organics, including: (1) the direct action of UVC photons (200–280 nm) on the oxidation of organic molecules [*Schuerger et al.*, 2011; *Stoker and Bullock*, 1997], (2) the formation of volatile oxidants (e.g., H$_2$O$_2$, O$_3^-$, O$^-$) from the interactions of UV light and Martian regolith with the subsequently produced oxidants causing the primary degradation of the organics [*Garry et al.*, 2006; *ten Kate et al.*, 2006; *Oró and Holzer*, 1979; *Yen et al.*, 2000; *Zent and McKay*, 1994], and (3) a photocatalytic process that occurs when UVA photons (320–400 nm) activate metal oxides in Martian regolith that subsequently degrade organics [*Shkrob et al.*, 2010].

[5] Recent studies have confirmed the evolution of methane from UV-irradiated organics under simulated Martian conditions [*Keppler et al.*, 2012; *Schuerger et al.*, 2011; *Stoker and Bullock*, 1997] and lab conditions relevant to Mars [*Shkrob et al.*, 2010]. First, *Stoker and Bullock* [1997] demonstrated the production of methane from UV-irradiated glycine, either alone (low CH$_4$ yield) or mixed into a Mars analog soil (high CH$_4$ yield), under simulated Martian conditions of 50–100 mbar, 24°C, equatorial UVC flux, and a Mars gas mixture. *Stoker and Bullock* [1997] concluded that the accreting organics from IDPs and carbonaceous chondrites might be degraded fast enough to eliminate most of the accreting organic carbon on an annual basis. Second, *Shkrob et al.* [2010] demonstrated that a UVA induced photo-Kolbe reaction (i.e., a photo-induced decarboxylation reaction) at mineral surfaces containing iron (III) oxides or TiO$_2$ can degrade a diversity of organic compounds and subsequently yield CH$_3^-$. The methyl radicals were then able to abstract H$^+$ ions from organic molecules to yield the volatile compound CH$_4$. Third, *Schuerger et al.* [2011] expanded on the work of *Stoker and Bullock* [1997] by testing the UV-induced evolution of methane from 15 organic compounds under simulated Martian conditions,

including pressures down to 6.9 mbar. In all cases, CH$_4$ was detected by *Schuerger et al.* [2011] from the UV-exposed organic compounds under Martian conditions with the highest production rate observed for the polycyclic aromatic hydrocarbon (PAH) pyrene (0.175 nmol g^{-1} h^{-1}), and the lowest rate observed for a Mars Exploration Rover (MER) spectral reflectance target (0.00065 nmol cm^{-2} h^{-1}). Methane was not detected from the UV-irradiation of two inorganic sources of carbon (i.e., CaCO$_3$ and graphite) leading the authors to conclude that the methane was derived directly from UV-irradiated organic compounds and did not involve atmospheric photochemistry within the Mars simulator. And, *Keppler et al.* [2012] demonstrated the evolution of methane from carbonaceous chondrites under simulated Martian conditions.

[6] The Mars UV/CH$_4$ studies by *Schuerger et al.* [2011], *Shkrob et al.* [2010], and *Stoker and Bullock* [1997] are consistent with terrestrial-based work that demonstrates methane, ethane, ethylene, and CO$_2$ are generated by the UVA irradiation (350 nm) of plant tissues [*McLeod et al.*, 2008; *Vigano et al.*, 2008]; and the production of CH$_4$, CO$_2$, and CO from UVA-induced (350 nm) photocatalytic reactions of C1–C3 alcohols in the presence of TiO$_2$ [*Dey and Pushpa*, 2006]. In all cases, methane was a direct by-product of the UV irradiation of organics under a wide range of temperatures, gas compositions, and pressures. The primary objectives of the current research were to (1) characterize the production of methane from UV-irradiated carbonaceous chondritic material under simulated Martian conditions, (2) model the global methane budget on Mars using the UV/CH$_4$ mechanism, and (3) determine if carbonaceous bolides might be invoked to explain the episodic occurrence of methane plumes on Mars.

2. Methods and Materials

2.1. Mars Chamber and CH$_4$ Calibration

[7] A previously described Mars Simulation Chamber (MSC) (Figure 1) [*Schuerger et al.*, 2008, 2011] was used to characterize the evolution of methane from UV-irradiated chondritic materials under Martian conditions. Methane experiments were conducted at (a) an atmospheric pressure of 6.9 mbar (±0.1 mbar), (b) temperatures of −80, −10, or 20°C (±1°C), (c) UV irradiation from 200 to 400 nm, (d) simulated dust loading in the atmosphere of optical depth (*tau*) 0.1, and (e) a Mars atmospheric gas mixture of CO$_2$ (95.5%), N$_2$ (2.7%), Ar (1.6%), O$_2$ (0.13%), and H$_2$O (0.03%). The upper temperature limit of 20°C was chosen based on the modeling of *Haberle et al.* [2001] which demonstrated that Martian surface temperatures could exceed 290 K for a few hours each sol between 0 and 30°S latitude during the Martian austral summer, and thus, represented an upper temperature limit on the rate of methane evolution from UV-irradiated organics on Mars. Environmental conditions were selected based on published data from the Viking, Pathfinder, and Opportunity missions [*Golombek et al.*, 1997; *Kieffer*, 1976; *Owen*, 1992; *Spanovich et al.*, 2006].

[8] Ultraviolet (UV) irradiation was supplied by one xenon-arc UV-enriched lamp (model 6269; Oriel/Newport Instruments, Corp, Mountain View, CA, USA) and delivered 4.0, 6.2, and 16.0 W m^{-2} of UVC (200–280 nm), UVB
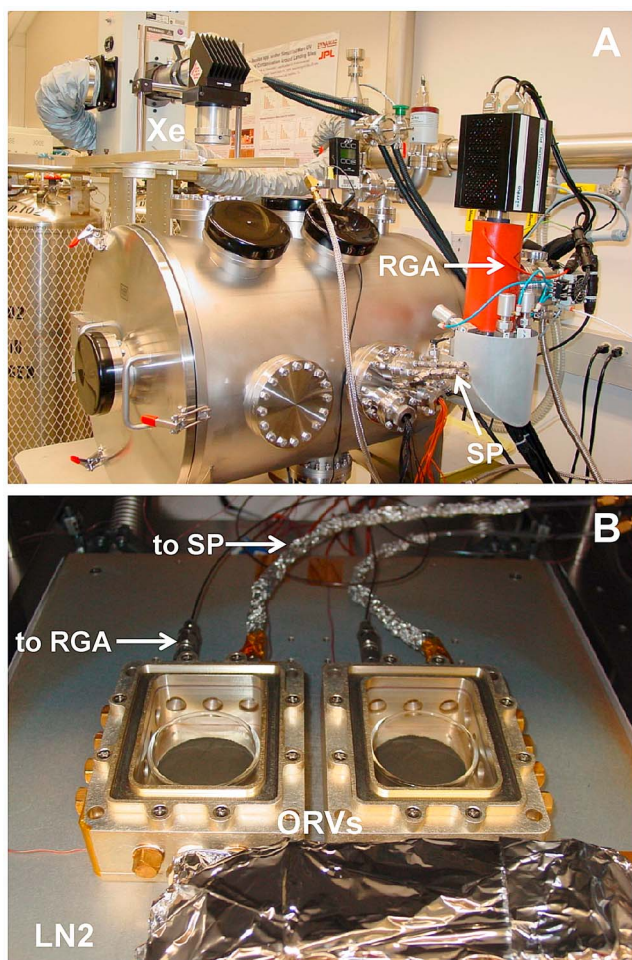
Figure 1. Mars Simulation Chamber (MSC). (a) The MSC system utilized a residual gas analyzer (RGA) to monitor the gas composition of the bulk Mars atmosphere. Methane-enriched gas samples were collected in Sulfinert® coated stainless steel vessels using the external sample ports (SP) on the right side of the MSC. (b) The Organic Reaction Vessels (ORVs) were mounted on the upper surface of the liquid nitrogen (LN2) thermal control plate. Gas lines on the back of the ORV units were plumbed to either the RGA (left-side lines) or the external sample ports (SP; right side lines).

(280–320 nm), and UVA (320–400 nm) irradiation, respectively, to the upper surfaces of the meteoritic samples. The UV flux and simulated *tau* of 0.1 were designed as a high UV irradiation scenario for equatorial Mars, under dust-free sky conditions, and at the mean orbital distance from the Sun [see *Schuerger et al.*, 2003, 2006]. Visible (VIS; 400–700 nm) and near-infrared (NIR; 700–1100 nm) irradiation were measured previously at 240 and 245 W m^{-2}, respectively [*Schuerger et al.*, 2003, 2006, 2011].

[9] Meteoritic samples were placed in borosilicate glass dishes (5-cm in diameter) and inserted into two Organic Reaction Vessels (ORVs) (Figure 1b) mounted to the upper surface of the LN2 thermal control plate within the MSC system. The ORV units were constructed of milled aluminum and coated with a chromate conversion film called chemfilm (Military-spec, C-5541F; also called alodine- or iridite-treated aluminum; *Schuerger et al.*, 2005). Two separate gas lines were connected to the rear of each ORV unit (Figure 1b), in which the left-side gas lines were connected to an external Residual Gas Analyzer (RGA), and the right-side gas lines were connected to external gas sample ports (Figure 1b). The right-side gas lines were used to both flush the ORVs with fresh Mars gas prior to initiating each experimental run (inbound gas flow), and then were used to sample the methane-enriched Mars gas at the completion of each test (outbound gas flow). To assist in coordinating the gas flow into and out of the ORV units, and in sealing the ORV internal void spaces (112 cm^3) from the bulk atmosphere within the Mars chamber ($\sim$0.14 m^3), individually controlled solenoid valves were placed on the front sides of both ORV units. The ORV surfaces were extensively cleaned and rinsed with 100% ethanol and filter-sterilized (0.22 μm pore size polyethersulfone membrane filters) double-deionized (18 Ω) water, respectively.

[10] The operation and calibration of the ORV units were extensively described in a previous paper on the production of methane from UV-irradiated spacecraft organics [*Schuerger et al.*, 2011]. In brief, crushed samples of meteorites were individually tested by placing 1-g aliquots into borosilicate glass dishes and inserting one dish into each ORV unit. The ORVs were closed, the Mars chamber sealed, and all components equilibrated for a minimum of 1 h at the Martian conditions required for each test. During the 1-h equilibration period, the internal ORV atmospheres were flushed with fresh Mars gas delivered via gas lines from the external side ports on the MSC (Figure 1a). Once the ORVs were equilibrated to a desired set of experimental conditions, UV irradiation was allowed to enter the MSC and ORV systems striking the upper surfaces of the crushed meteoritic samples. After either 8- or 16-h of UV irradiation (see section 2.3.), methane-enriched samples from ORV internal atmospheres were collected separately in pre-evacuated (<0.01 mbar) 75 ml Sulfinert™-treated stainless steel cylinders. Gas samples were analyzed with a Perkin Elmer Clarus 500 gas chromatograph (GC) (Waltham, MA, USA) equipped with a flame ionization detector and optimized for methane detection. Calibration of the ORV sampling and UV-irradiation procedures [*Schuerger et al.*, 2011] indicated that (1) the accuracy of the methane measurements was approximately ±0.5 ppm, (2) methane in the ORV headspace was degraded by UV irradiation at the rates of 5.8 and 9.5% for 8- or 16-h UV irradiation time steps, respectively, and (3) clean ORV units without meteoritic samples yielded background concentrations of 2.8 ppm methane after 8 h of UV irradiation (i.e., 1.2 ppm methane from the Mars gas, and 1.6 ppm from residual organics on surfaces of cleaned ORV units). Methane background and degradation rates were factored into estimating the methane evolution rates from UV-irradiated meteoritic samples under Martian conditions.

2.2. Preparation of Meteoritic Samples

[11] Four chondrites were selected to represent a range of properties from volatile poor, ordinary stony chondrites to carbonaceous chondrites with varying organic compositions. The chondrites were NWA 869 (L3–6), NWA 852 (CR2), Allende (CV3), and Murchison (CM2). All meteorite samples were crushed in separate clean ceramic mortar and pestles and dry sieved through cleaned 125-μm stainless

steel mesh screens. Crushed and sieved aliquots (3 mg) of each chondrite were analyzed for total carbon and inorganic carbon by, respectively, combustion at 950°C in pure oxygen (Perkin Elmer CE-440 Elemental Analyzer; by Galbraith Laboratories, Inc., Knoxville, TN, USA), and acid hydrolysis followed by carbon dioxide coulometry (CM 5014 Carbon Dioxide Coulometer; by Galbraith Labs). The overall accuracy for organic carbon determination was ±0.02 wt% (Galbraith Labs). Analyses indicated that the NWA869, NWA852, Allende, and Murchison samples used here contained 0.17, 0.27, 0.43, and 1.69 wt% organic carbon, respectively (i.e., total C minus inorganic C). Each chondrite had a trace amount of inorganic carbon present at the rates of 0.0189, 0.056, <0.04, and 0.057 wt%, respectively. Henceforth, the use of the terms carbon or C will refer to organic carbon.

[12] All chondrites likely contained trace amounts of terrestrial organic contamination that may have contributed slightly to the evolution of methane during UV irradiation experiments under Martian conditions. However, because the 1.69 wt% of C found in the Murchison sample was a significant mass of organic C, and most terrestrial contamination of carbonaceous chondrites is on the order of ppm not wt% [Botta and Bada, 2002], terrestrial organic contamination was believed to be a minor factor. Furthermore, the global UV/CH4 model relies upon the assumption that IDP particles contained on average 10 wt% C [Flynn, 1996; Thomas et al., 1993], further diminishing the possible effects that trace terrestrial organics might have had on the evolution rates of methane from UV-irradiated organics.

2.3. Methane Evolution Experiments

[13] Three separate experiments were conducted to characterize the methane evolution from UV irradiated carbonaceous and ordinary chondrites under simulated Martian conditions. First, fresh 1-g samples of the crushed and sieved Murchison meteorite were placed within ORV units and assayed for the evolution of methane under UV irradiation at −80, −10, and 20°C. Samples were equilibrated for 1 h at the desired conditions within the Mars chamber, and then irradiated continuously for 24 h. Methane enriched gas samples were collected twice during each 24-h cycle (i.e., an 8-h sample collected at 5 P.M., and a 16-h sample collected at 9 A.M. the following morning). Gas samples were assayed as described above, the data corrected for background levels of methane (2.8 ppm deducted from each assay), and then scaled upwards for methane loss due to UV photolysis (see section 2.1) [Schuerger et al., 2011]. Data were analyzed by linear regression (PROC REG in the Statistical Analysis System (SAS), version 9.1, SAS Institute, Inc., Cary, NC, USA) ($P \leq 0.01$; experimental $n = 18$).

[14] Second, four different chondrites were assayed for methane evolution at 20°C, 6.9 mbar, a Mars atmosphere, and a UV equatorial flux for Mars. Methane enriched gas samples were collected twice during each 24-h cycle, as described above. Fresh 1-g samples of the Murchison, Allende, NWA852, or NWA869 were run separately and completely randomized during the assays. Data were normalized as described above and analyzed by linear regression (PROC REG in SAS) ($P \leq 0.01$; experimental $n = 26$).

[15] And third, a time course study was conducted in order to determine if methane evolution from the UV-irradiated

Murchison meteorite would decrease over time. Fresh 1-g samples of the crushed and sieved Murchison chondrite were placed within both ORV units and equilibrated 1 h at 20°C, 6.9 mbar, and Mars atmosphere. After UV exposures, methane enriched gas samples were collected twice daily (i.e., 8-h and 16-h samples) for 20 days. On days 6, 12, and 18 the Mars chamber was briefly repressurized to lab conditions, the Murchison samples stirred with heat-sterilized stainless steel spatulas, and the samples returned to the simulated Martian conditions. Data were normalized, as described above and plotted as daily methane evolution rates (experimental $n = 40$).

2.4. UV/CH4 Model for Mars

[16] Results from the UV-induced methane evolution experiments (section 2.3) were combined with a Mars UV model [Moores et al., 2007] to characterize methane release from accreted organics in IDPs and low-mass carbonaceous chondrite on Mars. The algorithm on which the Moores et al. [2007] Mars UV model is based has been used successfully for studies of Earth, Mars, and Titan atmospheres [Moores et al., 2007, 2008; Tomasko et al., 2005]. The Mars UV model estimates UV fluence rates at the bottom of a 1-dimensional Mars atmosphere containing CO_2, O_3, dust, and ice particles in two stratified levels. The Mars UV model itself consists of two distinct layers containing CO_2 and Mie-scattering particulates based upon Mars Pathfinder results [Tomasko et al., 1999; Johnson et al., 2003] and is consistent with airborne particulates observed by the Viking landers and MER rovers [Lemmon et al., 2004]. The Mars UV model also contains appropriate levels of ozone which are permitted to vary seasonally and by latitude throughout a Martian year according to the simulations of Lefèvre et al. [2004], and validated by the SPICAM instrument onboard the Mars Express spacecraft [Perrier et al., 2006]. The accumulated incident UV energy for a Martian year is calculated by estimating the incident UV flux for an optical depth of 0.5 at each latitude, and for 40 separate times during each sol at 10° intervals in solar longitude (L_s).

[17] In order to incorporate the laboratory results for methane evolution directly into the Mars UV model, two key assumptions were used depending upon the applicable case. In the case where the incoming UV flux was the limiting factor for photolysis (i.e., photon-limited scenario) it was assumed that the meteoritic samples were sufficiently thick (~1 mm) that no UV photons penetrated to the bottom surfaces of each material; i.e., that increasing the depth of the samples would not have resulted in higher yields of methane. Previous work has demonstrated that UV photons are not likely to penetrate below 500 μm in fine-grained unconsolidated soils [Schuerger et al., 2003]. As such, the Martian surface could be considered draped by a uniform layer of the carbonaceous material, and thus, the predicted flux of UV photons could be ratioed to the methane production rate. In contrast, if the potential evolution of methane exceeded the supply of organic carbon from meteoritic accretion then carbon was taken as the limiting factor and all the accreted carbon was assumed to be destroyed. In the second case, the production of methane was said to be carbon-limited. The carbon-limited case assumes that UV-photolysis on the laboratory samples would eventually convert all C present to volatile products like methane,
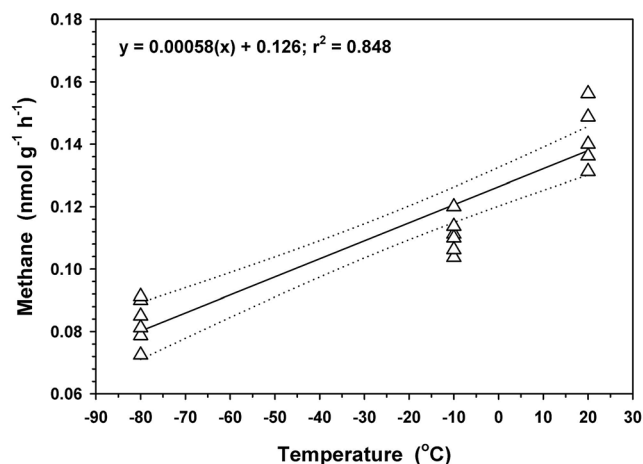
Figure 2. Effects of temperature on methane evolution from the Murchison meteorite under simulated Martian conditions (6.9 mbar; -80, -10, or $20°C$; Mars gas mix; Mars equatorial UV flux; *tau* of 0.1). Methane (CH_4) evolution from 1-g samples of the Murchison meteorite exposed to UV (200–400 nm) irradiation increased linearly as temperature increased. Data were best fit by a positively correlated linear model ($P \leq 0.01$; total n = 18; dotted lines are 95% CI). The average yield for CH_4 was 0.083, 0.111, and 0.145 nmol g^{-1} h^{-1} for samples irradiated at -80, -10, or $20°C$, respectively. Separate, and previously unexposed, aliquots of the crushed Murchison meteorite were used for each temperature. See section 3.1 for a discussion of the conversion rates of C to CH_4 by the UV/CH_4 linked process.

given sufficient time. However, the *carbon-limited* case does not mean that all C is destroyed instantaneously, but instead it presumes a steady state process in which the amount of organic carbon entering the system is balanced by an equal amount of carbon leaving the system.

[18] Based on the above discussion, the long-term methane production rates via the UV/CH_4 mechanism can be balanced relative to assumptions on the lifetime of atmospheric methane on Mars. Typical values for the methane lifetime reported in the literature are in the range of 250–670 Earth-years (henceforth years or Eyr) [*Atreya et al.*, 2007; *Lefèvre and Forget*, 2009; *Krasnopolsky et al.*, 2004; *Summers et al.*, 2002] which is much longer than the 1.88 terrestrial years of the Martian orbit. For long time periods of methane destruction (i.e., 300+ years), we consider the production rate of methane (0.024 nmol g^{-1} h^{-1}; section 3.1) at the end of a 20 day experiment (i.e., simulating 120 sols on Mars) for continuous UV irradiation of a Murchison sample with 1.69 wt% organic carbon. Similarly, the UV/CH_4 model may also be used to examine the maximum amplitudes of short-term methane plumes on Mars [e.g., *Mumma et al.*, 2009]. For modeling methane production of individual plumes, we selected the highest initial rate of methane production from fresh Murchison material (0.145 nmol g^{-1} h^{-1}; section 3.1) and lowered it over time to an asymptote of 0.024 nmol g^{-1} h^{-1} after 120 sol on Mars.

[19] In order to link methane production to UV flux, the efficiency of evolved methane (*EM*) per joule of UV energy must be defined. The *EM* can be expressed as the number of moles of methane produced per joule (J) of incoming UV

irradiation based on:

$$EM(\chi, T) = 2.76 \times 10^{-10} F_{CH4}[5.8 \times 10^{-4}(T - 273.15) + 0.126][6.9 \ \chi + 0.026] \quad (1)$$

where *EM* is expressed in mol J^{-1} and methane flux (F_{CH4}) is in units of nmol g^{-1} hr^{-1}. Carbon content (χ) is the mass fraction of organic carbon in the accreted material, and *T* is the temperature in K. For the case of material with 1 wt% carbon at 293 K, the value of *EM* corresponding to fresh material (i.e., using $F_{CH4} = 0.145$ nmol g^{-1} h^{-1}; from 20°C data in Figure 2) is $EM = 5.2 \times 10^{-13}$ mol J^{-1}. This value is similar to the results from *Stoker and Bullock* [1997] for glycine mixed with JSC Mars-1 palagonite for which the corresponding *EM* value is 4.1×10^{-13} mol J^{-1}. The total UV flux used here was based on earlier work by *Schuerger et al.* [2011], *Stoker and Bullock* [1997], and *Shkrob et al.* [2010]. However, separate UVC-only [*Schuerger et al.*, 2011; *Stoker and Bullock*, 1997] and UVA-only [*Shkrob et al.*, 2010] methane production processes may be jointly working on Mars and might yield different methane production rates for different spectral regions. It was beyond the scope of the current work to discriminate among methane production rates for specific UV bands.

[20] Several additional assumptions were incorporated into the UV/CH_4 model.

[21] (1) *Flynn* [1996] predicts the average accretion rate for carbon (C) to Mars via unaltered IDPs and small-mass carbonaceous chondrites (<1240 μm in diameter) as 2.4×10^5 kg per year. *Flynn et al.* [2010] demonstrate that the carbon present on IDP particles is primarily organic carbon and not amorphous inorganic carbon. Thus, the UV/CH_4 model assumes that the full mass of IDP carbon accreting to Mars is organic carbon.

[22] (2) Most carbon (90%) accreting to Mars is in the form of organics on IDP particles containing on average 10–12 wt% carbon [*Flynn*, 1996; *Flynn et al.*, 2010; *Thomas et al.*, 1993; *Schramm et al.*, 1989]. The *EM* from equation (1) was used to model the global methane budget based on a 10 wt% C content of accreted IDPs and small-mass carbonaceous chondrites.

[23] (3) Organics in IDPs occur as one of three types: (1) thin ∼50 to 200 nm rimes surrounding individual particles or aggregates of submicron particles, (2) a *glue-like* matrix that binds submicron mineral grains together, or (3) as discrete submicron- to micron-sized carbonaceous units within particles [*Flynn et al.*, 2003, 2010]. Second, *Jeong et al.* [2003] demonstrated that UVB and UVA photons can penetrate ∼180 nm, and UVC ∼40 nm, into Zn-oxide thin films; we assume similar depths for IDP organics. Third, *Schuerger et al.* [2003] demonstrated that UVC photons (down to 200 nm) can scatter around individual dust particles as large as 50 μm in diameter. And fourth, several mechanisms are likely involved in the breakup of IDP particles over time on Mars (e.g., partial ablation during reentry, mechanical shearing in dust storms, oxidant degradation, aqueous alteration in ice crystals), exposing fresh internal organic surfaces to UV degradation [*Moores and Schuerger*, 2012]. Thus, UV photons are assumed capable of accessing all surfaces of IDP organics over time when suspended in the Martian atmosphere or when

deposited as thin layers of individual particles on rock or regolith surfaces. For modeling purposes here, the idealized form of 200 nm organic rimes on IDP particles was used. We did not model burial of IDP or chondritic C in the regolith.

[24] (4) Ninety-percent of the UV photons in the Mars methane evolution experiments (section 2.3) were absorbed by the crushed meteoritic samples to depths down to 200 μm, with 100% of UV photons absorbed by the upper 500 μm of the 1-g samples (based on *Schuerger et al.* [2003]). Photon penetration is assumed to be possible by scattering through interstitial spaces within the unconsolidated crushed chondritic samples. Thus, the evolution of methane in the Mars chamber experiments was considered *photon limited*, and the Mars chamber experiments produced the maximum amount of methane possible for the simulated UV flux of the system.

[25] (5) A number of papers have demonstrated that CO_2, CO, NH_3, HCN, ethane, ethylene, and propane may be coevolved by UV irradiation of organics under conditions similar to those tested here [*Archer et al.*, 2010; *Dey and Pushpa*, 2006; *Ehrenfreund et al.*, 2001; *Keppler et al.*, 2012; *Oró and Holzer*, 1979; *Stoker and Bullock*, 1997]. However, the ratio of methane to the other coevolved volatiles is not well constrained for UV-irradiated carbonaceous materials under Martian conditions. Thus, we will model two cases for methane evolution from accreted carbon: (1) a theoretical upper limit in which 100% of accreted carbon is converted to methane, and (2) a lower range in which 20% of accreted carbon is converted to methane. The upper limit of 100% for converting C to methane via the UV/CH₄ process was chosen as a maximum theoretical limit on how much CH₄ can plausibly be added to the Martian atmosphere from IDP and small carbonaceous chondrites. The lower limit of 20% conversion was based on the following: (a) the H/C ratio of Murchison is 0.70 [*Naraoka et al.*, 2004] which would provide a 18.9% conversion rate if all H^+ in the organics were used in the UV/CH₄ process, (b) several atmospheric photochemical models predict H^+ radicals can be supplied to the atmosphere [*Krasnopolsky*, 2006; *Wong et al.*, 2003] possibly increasing the yields of CH₄ from UV-irradiated IDP organics, (c) volatile oxidants (e.g., H_2O_2, O_2^-, OH^-) are likely being generated on Mars [*Atreya et al.*, 2007; *Yen et al.*, 2000], and may add additional H^+ radicals to the regolith or atmosphere; and (d) *Stoker and Bullock* [1997] and *Keppler et al.* [2012] reported coevolution of several low-molecular weight organic volatiles at rates approximately 1-order of magnitude lower than methane, thus most organic volatiles from UV irradiated organics appear to be methane. Thus, a lower limit of 20% for the conversion of C to methane via the UV/CH₄ mechanisms was selected as a 1st-order low end-member. However, we acknowledge that the actual rate may be higher or lower than 20%, but empirical data are lacking to constrain the lower limit further.

[26] (6) *Flynn* [1996] argues that only IDP particles and low-mass chondrites with diameters less than 1240 μm can reach the Martian surface with unaltered carbon; and by implication, all chondrites larger than this limit lose all of the carbon to ablation. However, the geochemical condition of ablated carbon from carbonaceous chondrites >1240 μm in diameter is not well constrained, and will be ignored in the current UV/CH₄ model. If organics can be demonstrated to survive ablation and be available for conversion to methane by UV photons between 200 and 400 nm, the methane production rates from the UV/CH₄ model would increase.

[27] (7) Aside from the two end-member cases of *photon-limited* and *carbon-limited* behavior, methane production will vary slightly over the course of a year and with latitude as the UV flux and temperature change on shorter timescales than the typical lifetimes of accreted organics. This has no effect on the overall UV-photolytic rate, but does create small (parts per trillion) variations on diurnal and seasonal timescales. These minor variations are beyond the scope of the current paper, but are discussed in *Moores and Schuerger* [2012].

[28] (8) Although not tested here, the evolution of methane from organics was assumed to be positively correlated by a linear model to UV flux (confirmed by *Keppler et al.* [2012, Figure S3]).

2.5. Delivery of High Mass Carbonaceous Bolides to Mars

[29] We have investigated three possible scenarios for delivery of organics to the surface of Mars via asteroid or comet impacts and whether such events can explain the 45 ppbv methane plumes as reported by *Mumma et al.* [2009] (henceforth, 45 ppbv plumes). The first scenario involved the impact of a single bolide which can deliver sufficient organics to explain the entire amount of methane in 45 ppbv plumes. Standard projectile-crater and crater-ejecta scaling relationships [*Melosh*, 1989; *Barlow*, 2005] were used in the analysis to determine if sufficient mass of organics could be deposited over the entire region encompassed by the plumes.

[30] A second scenario involved a single airburst event of a coherent carbonaceous asteroid or comet (e.g., a bolide of uniform density and bounded by a mineralogically coherent structure) undergoing complete disruption during its atmospheric passage. The resulting airbursts would distribute materials over large regions on the surface, depending on the altitude of disruption and the angle of entry. A recent survey of fresh impact structures on Mars [*Daubar et al.*, 2010] indicates that as many as 77 new impact events creating meter-scale sized craters, or larger, are occurring on Mars each year, and as many as 60% of these are airburst events.

[31] *Zahnle* [1992] derived an equation relating altitude (z) of an airburst to atmospheric and projectile characteristics:

$$z = \frac{H}{2} \ln \left[\frac{3\pi \Gamma H \sec^3\theta}{\rho_i m_i} \left(\frac{\rho_0}{g} \right)^2 \right] \qquad (2)$$

where H is the atmospheric scale height (10.8 km for Mars), Γ is the drag coefficient of the atmosphere (~0.41 for Mars [*Desai et al.*, 2005]), ρ_i is the initial density of the projectile, p_0 is the atmospheric surface pressure (690 Pa; 6.9 mbar), g is the surface gravity (3.71 m s^{-2}), m_i is the initial mass of the projectile, and θ is the impact angle measured from the normal to the surface. Models were run for various combinations of ρ_i (100 to 400 kg m^{-3}) and θ (10° to 80° off nadir) for projectiles with radii from 30 to 100 m. The area covered by debris from an airburst at a specific altitude was estimated
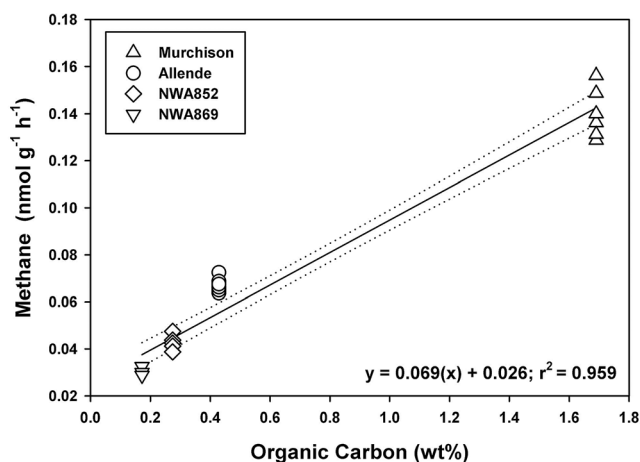
Figure 3. Methane (CH_4) evolution from four chondrites exposed to UV (200–400 nm) irradiation under simulated Martian conditions (6.9 mbar; 20°C; Mars gas mix; Mars equatorial UV flux; *tau* of 0.1). The percent organic carbon in each meteorite was analyzed by subtracting the inorganic carbon (derived from acid hydrolysis and carbon dioxide coulometry) from the total carbon (derived from combustion at 950°C in pure oxygen). Data were best fit by a positively correlated linear model ($P \leq 0.05$; total n = 26; dotted lines are 95% CI), with the amount of CH_4 evolved by UV photolysis correlated to the concentration of organic carbon in the samples. See section 3.1 for a discussion of the conversion rates of C to CH_4 by the UV/CH_4 linked process.

from the effective cross-sectional area ($s(z)$) of the swarm when it hits the surface (adapted from *Zahnle* [1992]):

$$s(z) = \frac{3\pi H}{\rho_i} \sec^2\theta \frac{p_0}{g} e^{z/H} \qquad (3)$$

[32] A third scenario was modeled that involved a low-density non-coherent carbonaceous bolide (e.g., a rubble-pile comet) fragmenting several times during atmospheric passage, with the spreading fragments undergoing further disruption during their transit to the Martian surface. Bolide fragmentation is commonly observed for meteoroids passing through Earth's atmosphere and the physics of meteoroid fragmentation and subsequent motion of the particles has been investigated for different planetary atmospheres [*Artemieva and Shuvalov*, 2001; *Popova et al.*, 2003; *Svetsov et al.*, 1995; *Zahnle*, 1992]. A bolide begins to fragment when the stagnation pressure of the airflow equals the compressive strength (σ_c) of the meteoroid [*Svetsov et al.*, 1995] following the relationship given by:

$$\sigma_c = \rho(z)v^2 \qquad (4)$$

where $\rho(z)$ is the atmospheric density at altitude z and v is the projectile velocity. We modeled several scenarios involving asteroids and comets to determine if multiple fragmentations could deposit the organics from bolides of varying sizes and densities over the area of the 45 ppbv plumes. Although the entire mass of an airburst is not likely to settle immediately below the atmospheric impact location of the bolide, general

circulation models (GCM) for wind patterns on Mars were ignored for the current study.

3. Results

3.1. Methane Evolution From UV-Irradiated Meteoritic Samples

[33] In all three Mars chamber experiments outlined below, no evidence was observed for the coevolution of other low molecular weight organic volatiles in the gas samples besides methane. The GC-column and flame-ionization detector on the GC were adequately sensitive to have detected organic volatiles up to C_3 compounds including acetylene, ethane, ethylene, and propane down to 0.5 ppm, but failed to do so. The GC flame-ionization detector was not sensitive to the possible coevolution of CO or CO_2.

[34] The UV-irradiation of crushed Murchison samples under simulated Martian conditions yielded methane at the rate of 0.145 nmol g⁻¹ h⁻¹ at 20°C, but decreased to 0.083 nmol g⁻¹ h⁻¹ at −80°C (Figure 2). The relationship between methane evolution and temperature was best described by a linear model (y = 0.00058(x) + 0.126; r² = 0.848). No visually obvious changes in the weight or the physical appearance of the Murchison samples were observed following exposure to Martian conditions (data not shown). The concentrations of methane evolved during 24-h assays were observed to be positively correlated to the amount of carbon in each of the four meteoritic samples tested (i.e., Murchison, Allende, NWA852, and NWA869) (Figure 3). The methane produced versus the weight percent carbon in the meteorites was best described by a linear model (y = 0.069(x) + 0.026; r² = 0.959). The methane production rate (0.141 nmol g⁻¹ h⁻¹) observed for a fresh Murchison sample in Figure 3 was very similar to the methane production rate observed for the fresh Murchison sample in Figure 2, confirming the precision of the experimental protocols. The lowest methane production rates were observed for the meteorites NWA852 and NWA869 (0.042 and 0.030 nmol g⁻¹ h⁻¹, respectively). The relationships between evolved methane and UV-flux with respect to temperature and carbon content are included explicitly in equation (1) that describes the efficiency of evolution of methane (*EM*) by the UV/CH4 process.

[35] In a separate time-course study on the evolution of methane under Martian conditions, the initial methane evolution rate from fresh Murchison samples was 0.126 nmol g⁻¹ h⁻¹ for the first 24-h time step, but decreased over time approaching an asymptote of approximately 0.024 nmol g⁻¹ h⁻¹ after 20 d of continuous UV irradiation under Martian conditions (i.e., simulating 120 sols on Mars; Figure 4). When the Murchison samples were mixed on days 6, 12, and 18, the methane evolution rates jumped 49, 38, and 35%, respectively, relative to the premixed time step. The exponential decay curve for Figure 4 was fit best by the equation:

$$F_{CH4}(t) = (0.145 - 0.024)e^{\left(-\int_0^t F_{UV}dt / E\right)} + 0.024 \qquad (5)$$

where, $F_{CH4}(t)$ is the methane flux in the ORVs expressed in nmol g⁻¹ hr⁻¹. F_{UV} is the ultraviolet flux between 200 nm and 400 nm in the ORVs; held constant at 26.2 W m⁻². The
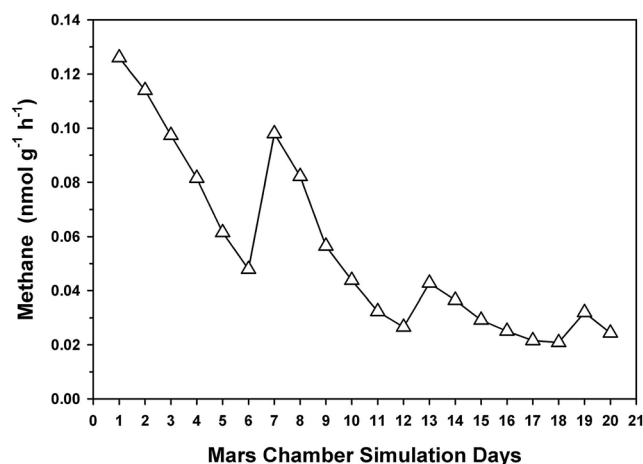
Figure 4. Time-course experiment on the evolution of methane (CH_4) from 1-g samples of the Murchison meteorite exposed to UV (200 to 400) irradiation under simulated Martian conditions (6.9 mbar; 20°C; Mars gas mix; Mars equatorial UV flux; optical depth (*tau*) of 0.1). The Murchison samples were stirred on days 6, 12, and 18. Results indicate that after each mixing event, the CH_4 would increase significantly due to new reactive sites being exposed on the meteoritic organic molecules for UV photolysis, but then subsequently decrease over time under continued UV exposure. The overall trend in CH_4 evolution appeared to approach an asymptote at approximately 0.024 nmol g^{-1} h^{-1} (points are means of two replicates; total n = 40). Each Earth day in the Mars simulator (*tau* 0.1) equaled 5.5 sols on equatorial Mars at a nominal *tau* of 0.5 [*Moores et al.*, 2007]. The exponential decay curve was fit best by equation (5). See section 3.1 for a discussion of the conversion rates of C to CH_4 by the UV/CH_4 linked process.

exponential decay constant, *E*, produced a good fit when set at 9×10^6 J m^{-2}.

[36] Based on the data in Figures 2, 3, and 4, the *EM* for a Murchison sample at 1.69 wt% under Martian conditions was estimated at 7.9×10^{-13} mol J^{-1} for model scenarios run at 20°C, 6.9 mbar, and a UV flux of 26.2 W m^{-2}. At temperatures closer to −80°C, the *EM* would be 4.5×10^{-13} mol J^{-1} for Murchison-like levels of organics. For IDP organics at 10 wt% C, the *EM* would range between 2.3×10^{-12} to 3.9×10^{-12} mol J^{-1} for temperatures −80 to 20°C, respectively.

[37] What is the conversion rate of C to CH_4 over 20 days based on the results in Figure 4? The 1-g Murchison samples used to generate data in Figure 4 were ~1 mm deep. The amount was chosen to assure that 100% of all UV photons would be absorbed by organic and mineral components in the sample. Over the course of the 20-d experiment, curve fitting the data (equation (5)) and assuming no spikes yields 29 nmol of methane evolved; or 3.49×10^{-7} g C was converted to CH_4. By assuming (1) a UV penetration depth of 180 nm (based on *Jeong et al.* [2003]) yielding a volume of material exposed to UV photons of 4.2×10^{-10} m^3, (2) a density similar to water (1000 kg/m^3), (3) organic content of the Murchison at 1.69 wt%, (4) a surface area of the UV irradiated sample of 0.0021 m^2, and (5) a UV fluence rate of 26.2 W m^{-2} yields a conversion rate of 5.5% of C to CH_4

over 20 days. We must emphasize that the value of 5.5% does not represent the conversion rate for the entire 1 g of material over 20 days, but only for the volume of material down to a depth of 180 nm in all organic surfaces that were struck by UV photons. For example, if the 1-g samples were spread over larger areas, additional methane would have been measured from the 1-g samples (confirmed by the spikes in Figure 4 when the samples were stirred). Thus, the conversion rate of 5.5% over 20 days is considered a lower bound estimate on how much methane might be evolved from all materials if every surface were equally exposed to UV photons. For the modeling presented below, a 20% conversion rate is retained as a lower bound end-member for all organics based primarily on an H/C ratio of 0.70 for Murchison [*Naraoka et al.*, 2004], which implies a conversion rate of 18.9% if all H$^+$ in the organics were consumed by the C to CH_4 photolytic pathways. Rounding up to 20% is also justified by the likely possibility that additional H$^+$ ions from other photochemical pathways in the Martian atmosphere and regolith [*Krasnopolsky*, 2006; *Wong et al.*, 2003; *Yen et al.*, 2000] would be available for the UV/CH_4 process; and secondary coevolved species like ethane, propane, ethylene, propylene are produced at less than 10% of the rate that methane is evolved from UV irradiated organics [see *Keppler et al.*, 2012; *Stoker and Bullock*, 1997]. And lastly, the global modeling of methane from accreted organics (see section 3.2) assumes that numerous mechanical and physical processes are present on Mars [see *Moores and Schuerger*, 2012] that eventually permits UV photons to interact with all organics as the IDP and small chondrites are degraded over time.

3.2. UV Photolysis of Accreted Carbon

[38] The Mars UV model [*Moores et al.*, 2007] predicts that the UV fluence rate will be highest between 0° and 45°S latitude during the austral summer at solar longitudes (*L*$_s$) of 225° to 325° (Figure 5). The UV flux per sol averages 1.3×10^6 J m^{-2} sol^{-1} over the year at the equator, and decreases to approximately 6.7×10^5 J m^{-2} sol^{-1} at 80°N or S latitude over the year and considering only sunlit days. The UV flux varies by ±20% from the daily average throughout the Martian year near the equator due to the inclination of the rotational axis and the eccentricity of the orbit.

[39] Most organic carbon arrives at the surface of Mars as accreted IDPs (>90%) [*Flynn*, 1996] which have an average carbon content of ~10 wt% [*Schramm et al.*, 1989; *Thomas et al.*, 1993]. As such, it is possible to apply equation (1) to the total UV flux at the surface of Mars to determine whether evolution of methane from organic material is *photon-limited* or *carbon limited*. We modeled a range of 20% to 100% conversion of UV-irradiated organics to methane. The rate of accreted IDP organics converted to methane per year was modeled to range between 3.3×10^{-10} kg m^{-2} (20% conversion) and 1.6×10^{-9} kg m^{-2} (100% conversion) (Figure 6). In contrast, the mass of carbon capable of being converted to methane by the action of all UV photons striking the surface (from Figure 5) was observed to range between 2.2×10^{-5} kg m^{-2} yr^{-1} for fresh carbon near the equator (i.e., based on 0.145 nmol g^{-1} h^{-1} of CH_4 evolution at 20°C; Figure 2) and 5.9×10^{-7} kg m^{-2} yr^{-1} near the poles (i.e., based on the asymptotic rate of 0.024 nmol g^{-1} h^{-1} methane evolution after 20 d of UV exposure; Figure 4).
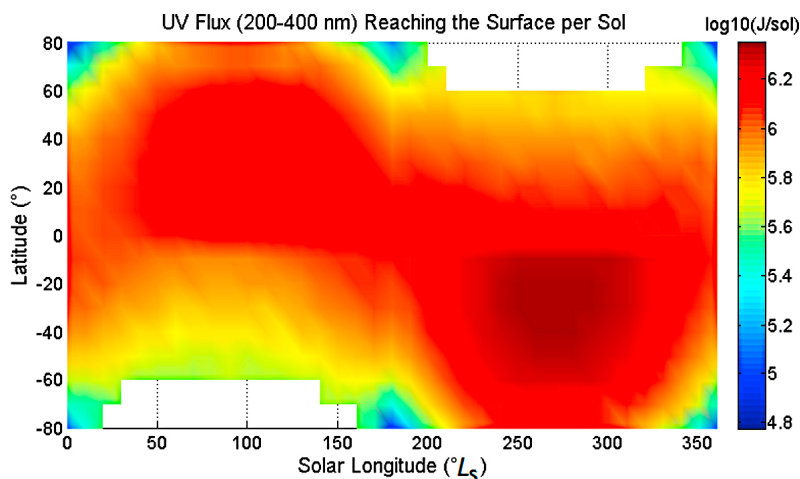
Figure 5. Ultraviolet (UV; 200–400 nm) fluence rates for local noon on daytime Mars at an optical depth (*tau*) of 0.5. Units are in $\log_{10}$ joules per sol (J sol^{-1}), and are modeled for latitude and solar longitude (L_s). Values range from zero during polar winter to 2.2×10^6 J sol^{-1} near southern summer solstice between 20°S and 30°S and L_s of 225° to 325°.

From Figure 6 it is apparent that for all latitudes on Mars there is sufficient UV to destroy in excess of three orders of magnitude more organic carbon as arrives on the surface through accretion, even if we assume that 100 wt% of carbon is converted to methane. Thus, the UV-induced conversion of organic carbon to methane on Mars can be considered to be *carbon-limited*.

[40] Methane production from the UV irradiation of accreted organics can be converted to an atmospheric concentration by assuming complete vertical mixing in the atmosphere, and by assuming a given ratio of organics converted to methane per year. If a pressure of 6.9 mbar is used, each 1 ppbv of methane represents 4.2×10^{-6} mol m^{-2} of CH₄ which contains 5.1×10^{-8} kg m^{-2} of carbon. Thus, if the total organic accretion rate of 2.4×10^5 kg C yr^{-1} was equally distributed over the Martian surface and 20 to 100% of the material photolyzed by UV and converted to methane, concentrations between 0.0064 and 0.033 ppbv methane, respectively, would be added to the Martian atmosphere per year. These input rates would generate between 64 and 320 t of methane per year for the 20 to 100% conversion rates, respectively. Furthermore, these annual
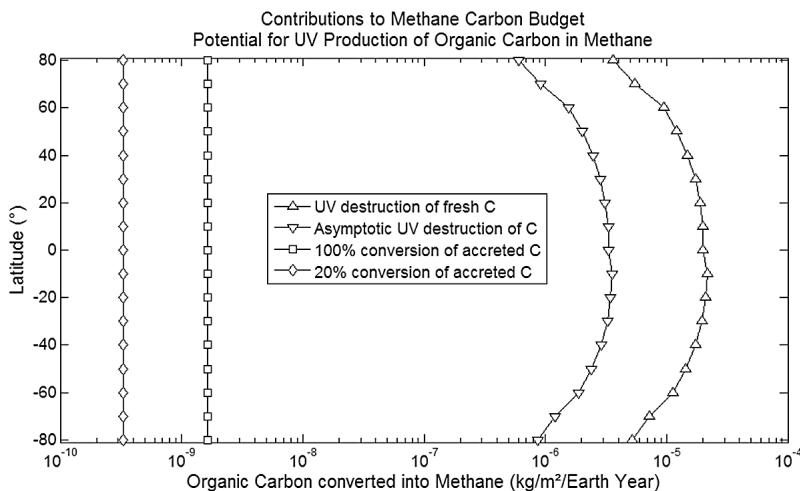

Figure 6. Annual totals for accreting carbon and UV destruction potential by latitude in kg m^{-2} per year. The range for UV destruction potential is shown with triangles (right two plots) with the lower and upper limits representing the asymptotic methane production rate (0.024 nmol g^{-1} h^{-1}; from Figure 4) and the freshly exposed methane production rate (0.145 nmol g^{-1} h^{-1}; from Figure 2). The two left-hand plots show the range of IDP and meteoritic accretion assuming that the accretion is isotropic over the surface and the lower limit correspond to 100 wt% conversion of all organic carbon to methane (squares) and 20 wt% converted to methane (diamonds). Under all circumstances, UV destruction potential is several orders of magnitude higher than the amount of available carbon. Therefore, the production of methane via the UV/CH₄ mechanism remains *carbon-limited* on Mars.
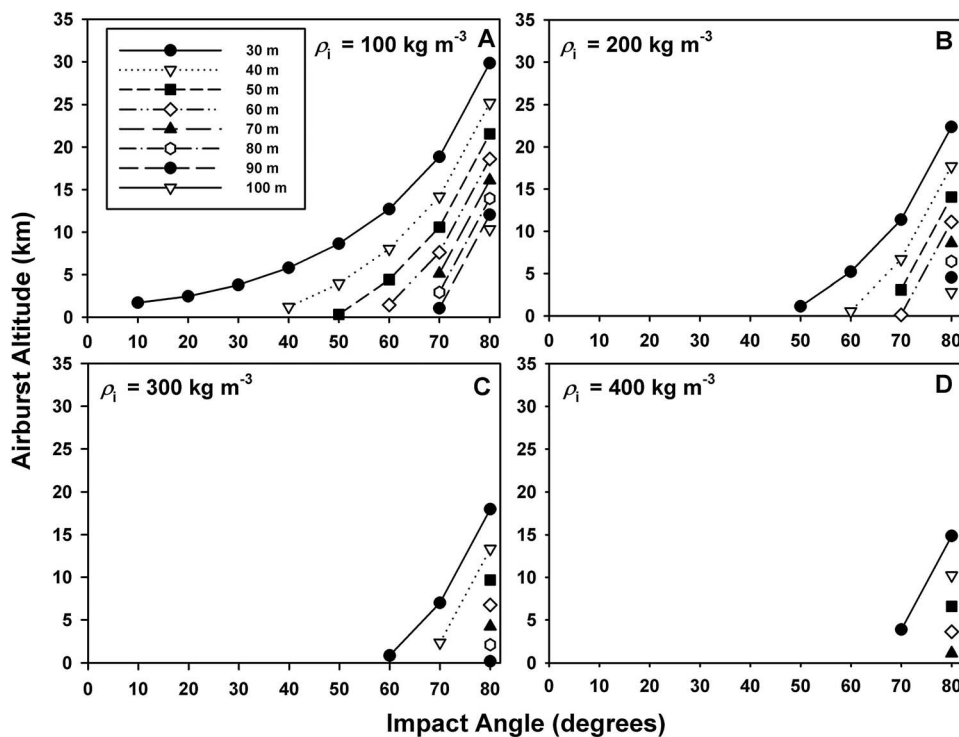
Figure 7. Airburst altitudes versus impact angles for coherent bodies at uniform densities (ρ_i) of (a) 100, (b) 200, (c) 300, and (d) 400 kg m^{-3}. Radii (legend box) were varied from 30 to 100 m. The highest airburst altitude of 30 km is obtained for a 30-m radius bolide entering the Martian atmosphere at an angle of 80° off-nadir. Coherent bodies with densities higher than 400 kg m^{-3} or radii larger than 100 m did not undergo airbursts before striking the Martian surface.

production rates for methane by the UV/CH$_4$ process predict uniformly distributed global averages between 2.2 and 11 ppbv accumulated over geological time for 20 and 100% conversion rates, respectively, if the destruction rate of methane is 329 terrestrial years [*Lefèvre and Forget*, 2009].

3.3. Bolide Impacts on Mars

[41] The UV/CH$_4$ model of isotropically accreted IDP organics can explain a globally averaged methane concentration of 2.2 to 11 ppbv for 20 to 100% conversion rates of UV-irradiated organics to methane, respectively. However, the UV/CH$_4$ model for IDP carbon is unable to produce plumes of significant strength (i.e., up to 45 ppbv) due to the relatively slow rate at which IDP carbon is supplied to the system (Figure 6). For example, the steady supply of IDP carbon to Mars is only 4.7×10^{-12} kg m^{-2} sol^{-1} which predicts a mean daily global methane production of only 0.09 pptv per sol. However, if organics were suddenly increased in a single event, larger plumes of methane might be observable. One possible mechanism that might yield a sudden increase of organic carbon at the Martian surface would be an impact or airburst event of a carbonaceous bolide with high carbon content. We model here the mass (1.8×10^9 kg) and areal (9×10^6 km^2) constraints for matching the 45 ppbv methane plumes, and in section 3.4 we model the conversion of dispersed organics to methane by the UV/CH$_4$ process.

[42] Distribution of organics by a single crater-forming impact is unlikely to distribute the bolide organics over the

9×10^6 km^2 region required to match the 45 ppbv methane plume reported by *Mumma et al.* [2009]. The temperatures and pressures associated with projectile destruction and crater formation would likely destroy the organics prior to their distribution over the surrounding region. Furthermore, ejecta deposits surrounding the crater are largely derived from the target (planet) rather than the projectile, so any surviving organics would be thinly distributed within the ejecta blanket, and likely not fully exposed to solar UV irradiation. The area of the methane signature also is quite large—for this area to be covered with a continuous ejecta deposit (which typically extends 1.5–2.0 crater radii from the crater rim [*Barlow*, 2005]) would require that a crater over 1000 km in diameter be formed in the 2002–2003 time period. Considering a discontinuous ejecta blanket from a smaller bolide, (which can extend up to 100–200 crater radii from the rim [*Tornabene et al.*, 2006; *Preblich et al.*, 2007]), would still require a crater 10–20 km in diameter. Comparison of images taken by orbiting spacecraft between 1976 and the detection of the plumes in 2003 do not reveal any newly formed craters in these size ranges [*Malin et al.*, 2006], and thus, a single bolide impact event cannot explain methane plumes on Mars.

[43] We have calculated the airburst altitudes for coherent low-density bolides ranging in radii from 30 m to 100 m, and with initial densities from 100 kg m^{-3} to 400 kg m^{-3} using equation (2). Results indicate that the highest airburst altitude (30 km) is obtained for the smallest object (30 m radius) with a very low ρ_i (100 kg m^{-3}) and high θ (80°) (Figure 7).

However, a bolide of this size shattered by an airburst at 30 km would supply only 1.13×10^7 kg of material (from equation (3)) (versus the required mass of 1.8×10^9 kg), and would not spread the organic-rich debris over a wide enough area (only 1.02×10^2 km^2 versus the required 9×10^6 km^2) to match the spatial characteristics of the 45 ppbv plumes described by *Mumma et al.* [2009]. Thus, a single airburst event of a low-density coherent bolide cannot explain the methane plumes on Mars.

[44] For a higher altitude airburst event, a non-coherent and low-density bolide, fragmenting several times during reentry (e.g., rubble-pile comet) is required. Equation (3) demonstrates that such a bolide must be disrupted initially at an altitude of ~150 km for the debris to cover an area of 9×10^6 km^2. Furthermore, the compressive stresses for carbonaceous chondrites vary and can range from 10^5 Pa to 2.5×10^6 Pa [*Popova et al.*, 2003]. Using the lower value of 10^5 Pa and an average asteroid impact velocity at Mars of 9.3 km s^{-1} [*Steel*, 1998] gives an atmospheric density of 1.16×10^{-3} kg m^{-3} when the carbonaceous bolide will begin to fragment. This corresponds to an altitude of about 30 km on Mars, which, as noted above, is too low for the debris to cover the required 9×10^6 km^2 area of the 45 ppbv plumes. However, non-coherent internal structures of comets can have lower material strengths, and may be composed of diverse materials forming a sort of rubble-pile held loosely together by internal gravity. Studies of the tidal disruption of Comet Shoemaker-Levy 9 suggest that the material strength of a 10-km-diameter rubble-pile comet is ~10^3 Pa [*Svetsov et al.*, 1995]. Using this value and an average cometary impact velocity of 45 km s^{-1} at Mars [*Steel*, 1998] indicates that a non-coherent rubble-pile comet can begin to fragment at an atmospheric density of 4.9×10^{-7} kg m^{-3}, corresponding to an altitude of ~115 km. Oblique entry angles would cause greater stresses on the comet which could cause it to begin fragmentation at higher altitudes, approaching the ~150 km altitude needed to distribute debris over the observed area of the methane plume. Further fragmentations (i.e., additional airbursts of smaller meteoroids) of the material are likely as the swarm continues its passage through the atmosphere, allowing for distribution of fine-grained organic material over large areas of the surface.

[45] To further investigate the rubble-pile comet scenario, we calculated the airburst heights of three pieces of a low-density (100 kg m^{-3}) comet necessary to distribute material across the regions of the *Mumma et al.* [2009] plumes A, B$_1$, and B$_2$. We assumed an entry angle θ of 80° since this produces the highest possible altitude of disruption and therefore gives the maximum coverage of debris across the surface. Plume A covers the region between approximately 25°S to 30°N latitude, and 30°E to 57.5°E longitude, which represents a surface area of about 5.0×10^6 km^2. Plume B$_1$ is associated with the region between 15°N to 35°N latitude, and 70°E to 85°E, representing an area of about 1.5×10^6 km^2. Plume B$_2$ is located in the region bounded by 7°S to 12.5°N latitude, and 63°E to 83°E longitude, which covers a surface area of approximately 2.0×10^6 km^2. Using equation (3), the fragment producing plume A would need to undergo an airburst at an altitude of ~150 km, while those fragments producing plumes B$_1$ and B$_2$ would need to be disrupted at altitudes of ~134 km and ~137 km, respectively. Thus, a debris field covering the necessary surface

area of the observed *Mumma et al.* [2009] methane plumes can be created by a high-altitude series of airbursts by a fragmenting rubble-pile comet, but requires very specific impactor conditions to do so.

[46] Is there any evidence that an airburst might have occurred in the region of the *Mumma et al.* [2009] methane plumes? The methane plumes were detected in 2003 during Martian summer (L_s = 121° to 155°), indicating that if they were produced by UV irradiation of cometary carbonaceous material that the associated impact/airburst must have occurred around this time period. *Malin et al.* [2006] report the formation of 20 new small impact craters on Mars between May 1999 and March 2006, as revealed by repeated observations from the Mars Global Surveyor Mars Orbiter Camera (MOC). And fragmentations of bolides as they pass through the Martian atmosphere appear to be a common occurrence on Mars, based on the number of newly formed crater clusters being detected by the Mars Reconnaissance Orbiter's High Resolution Imaging Stereo Experiment (HiRISE) (e.g., Figures 8a and 8b) [*Daubar et al.*, 2010]. One of these craters (Figure 8a; impact site 4 [*Malin et al.*, 2006]) is located between the three methane plumes (23.3°N 52.8°E) and formed in the time period between 4 February 2001 and 13 June 2005. High resolution images from the MOC and Mars Reconnaissance Orbiter High Resolution Imaging Stereo Experiment (HiRISE) reveal a 15.6 ± 1.7 m diameter crater surrounded by a dark halo with a bright elongated ejecta blanket (Figure 8a). The elongated ejecta blanket combined with the approximately circular appearance of the crater suggests that the impact angle was in the range $55° \leq \theta \leq 75°$ from vertical [*Herrick and Hessen*, 2006]. The dark halo surrounding the crater and ejecta deposit is similar to those seen around impact craters on Venus, which have been proposed to form from shock waves of airbursting impactors interacting with the ground [*Zahnle*, 1992]. Assuming an impact angle near 75° and using the crater models of *Melosh* [1989], the projectile diameter depicted in Figure 8a should be in the range of ~1.8 m with a mass of ~305 kg. The bolide diameter and mass are too small to account for the size of a single bolide required to generate a large methane plume similar to those reported by *Mumma et al.* [2009]. But if the impact is the remnant of a larger bolide that initiated an airburst at a higher altitude, it is plausible that an airburst occurred in the region near the 45 ppbv methane plume that overlaps in time with the methane plume reported by *Mumma et al.* [2009].

[47] The bolide impact modeling indicates that the only way to distribute carbonaceous debris over the area covered by the 45 ppbv methane plume is through multiple fragmentations of a 150-m low-density non-coherent rubble-pile comet as it passes obliquely through the Martian atmosphere, and with bolide disruption beginning at an altitude of ~150 km. If steeper entry angles are used, for example 45° or 60° off-nadir, then the 150-m diameter, 100 kg/m^3, non-coherent rubble-pile comet would not undergo an airburst at all, but would instead impact the surface. The minimum entry angle for any airburst scenario of the modeled 150-m comet is 64° off-nadir, with the airburst occurring very deep in the atmosphere near the surface of Mars. For similar low-density rubble pile comets, the modeling indicates that for 45°, 60°, or 80° off-nadir entry angles, the diameters must be <93 m, <131 m, or <378 m, respectively, to yield airbursts in
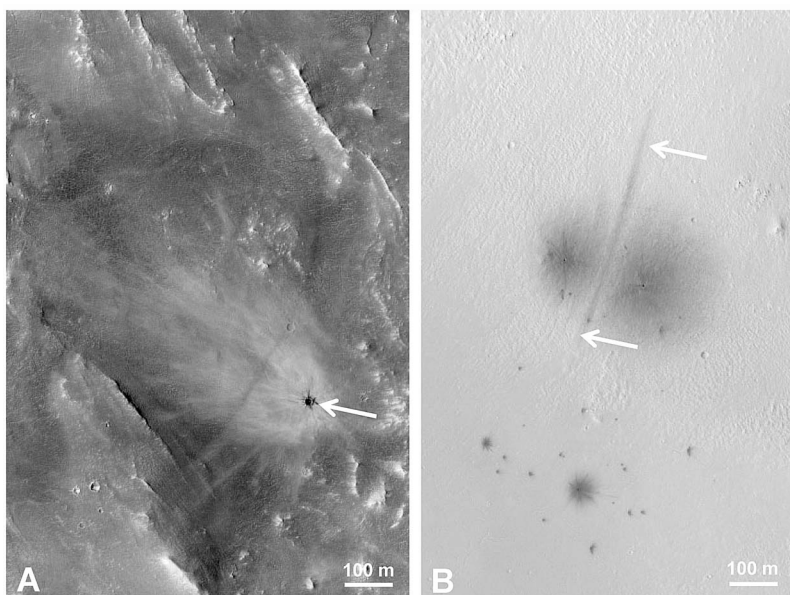
Figure 8. Cratering evidence for current day bolide airbursts on Mars. (a) Small (15.6 m diameter) crater formed between 4 February 2001 and 13 June 2005 in region of observed methane plumes [*Mumma et al.*, 2009]. The dark crater (arrow) centered at 23.3°N 52.8°E displays an elongated bright ejecta deposit surrounded by a dark halo (HiRISE image PSP_007003_2035), which appears similar to an airburst with a single fragment impactor as described for Venus [*Zahnle*, 1992]. (b) Dispersed crater cluster consisting of bolide fragments separated during passage through the Martian atmosphere between May 2003 and September 2007. Dark line (arrows) between the two largest fragments may have resulted from interaction of ejecta curtains during simultaneous impacts. The cluster is centered near 8.6°N 46.8°E (HiRISE image ESP_011618_1885).

the Martian atmosphere. Furthermore, if steeper entry angles and smaller sized comets were to create airbursts, the altitudes and debris fields would be significantly lower and smaller, respectively, than those required to achieve the areal distribution of the 45 ppbv methane plume. For example, for an entry angle of 45° off-nadir, a 90-m rubble-pile comet would create an airburst at only 520 m above the Martian surface, and distribute the debris field over an area of 0.403 km^2. For an entry angle of 60° off-nadir, a 130-m rubble-pile comet would create an airburst at only 177 m above the Martian surface, and distribute the debris field over an area of 0.781 km^2. Thus, the areal extents of debris fields decrease for all airburst scenarios that deviate from the 80° off-nadir, 150-m diameter, 100 kg/m^3, rubble-pile comet scenario modeled above.

[48] The airburst modeling indicates that the areal extent of the plumes observed by *Mumma et al.* [2009] can be reproduced only under a very specific set of circumstances. One small impact crater (Figure 8a) was formed near the plume locations during the time period which overlaps the plume detection in the summer of 2003, which might support the conclusion that an airburst occurred in the time and spatial constraints associated with the three methane plumes reported by *Mumma et al.* [2009]. However, the conditions required to deliver the required mass (1.8 × 10^9 kg) over the required area (9 × 10^6 km^2) from a carbonaceous bolide to match the physical plume characteristics reported by *Mumma et al.* [2009] appear to be extremely unusual, and thus, are unlikely to be frequent occurrences on Mars.

3.4. CH4 Generated From Bolide Impact or Airburst Events on Mars

[49] Assuming that an infrequent 150-m, low-density, rubble-pile comet airburst event did occur as described above, can the UV/CH4 process create the volume of methane (19,000 t) as reported by *Mumma et al.* [2009]? The plume models in Figure 9 were normalized for the effects of temperature on methane evolution from UV-irradiated organics (Figure 2), and for the range of UV fluence rates on Mars (Figure 5). Furthermore, data in Figure 9 are based on the exponential decay curve for methane in Figure 4 for fresh Murchison samples continuously irradiated with UV photons for 20 days under simulated Martian conditions. Based on the UV model of *Moores et al.* [2007], 20 days of continuous UV irradiation in our experiments approximates 120 sols on equatorial Mars. Depending on the specific temperature and diurnal UV flux at each latitude at each time of the year, the representation of the decay curve modeled by equation (5) was employed to determine the total amount of integrated methane produced over 120 sols.

[50] Figure 9a gives a theoretical maximum output of methane abundance for a carbonaceous bolide delivering sufficient mass to the Martian surface to create a *photon-limited* condition with organics at 1.69 wt% C (Murchison), 10 wt% C (average abundance for IDP or cometary organics; see *Chyba and Sagan*, 1992; *Flynn*, 1996; *Thomas et al.*, 1993), or 24 wt% C (high-end IDP-like mass for C; see *Thomas et al.*, 1993). The plume concentrations given in Figure 9a must be overlaid onto a global average of 2.2 to
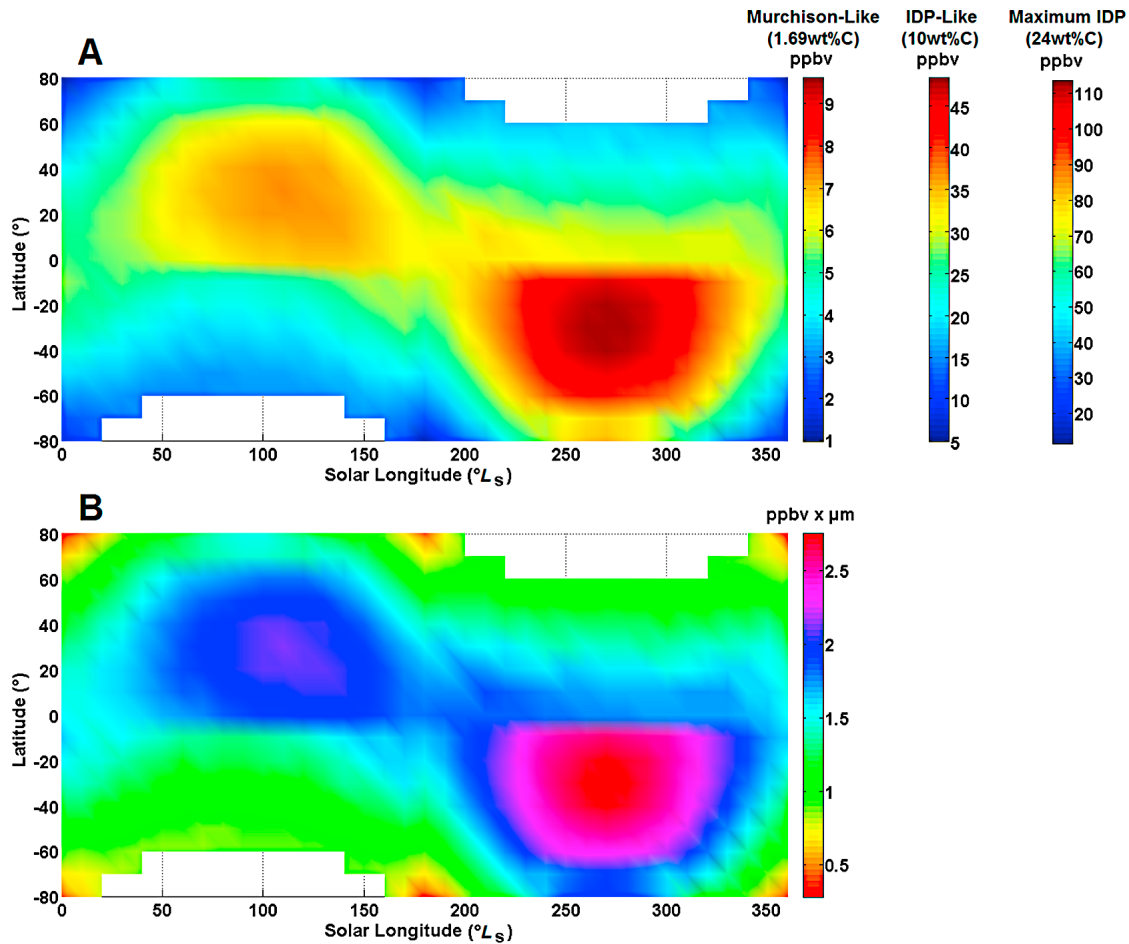
Figure 9. Enrichments in column methane abundance above background levels for airbursts derived from the UV photolysis of organic carbon under *photon-limited* conditions. (a) Theoretical high end-member for airbursts of non-coherent bolides (e.g., rubble-pile comets) measuring 150 m in diameter, masses of 1.8×10^9 kg, and with 11 wt% organic carbon. However, results are based on several unrealistic assumptions (see section 3.4), and thus, are unlikely to occur on Mars. (b) Effects of particle size on methane abundance in more realistic plumes created by airbursts of 150-m diameter, low-density (100 kg/m³), rubble-pile comets, and entry angles close to 80° off-nadir. The atmospheric methane abundance can be estimated by dividing the scale values in the legend by the assumed particle radius in microns.

11 ppbv to yield the measured methane abundance in a plume. For example, a 45 ppbv methane plume might be satisfied by a global average of 10 ppbv and a short-lived plume of 35 ppbv of methane. For the mass (1.8×10^9 kg) considered here, a bolide with 11 wt% C might yield a plume of suitable concentration (i.e., 35 ppbv plume + 10 ppbv background) and be dispersed over the required area (9×10^6 km²) of the *Mumma et al.* [2009] plumes if the following assumptions are satisfied: (a) 100% of the organics were converted to methane over 120 sols, (b) there was no mixing of the plume with the general atmosphere over 120 sols, (c) the total mass of the bolide was spread in a uniform 30-nm thick sheet over the 9×10^6 km², and (d) the 80° off-nadir entry angle, low-density, rubble-pile comet airburst scenario outlined in section 3.3 holds. These conditions are extreme, but are required to achieve a methane plume of 45 ppbv produced exclusively by the UV/CH₄ process over 120 sols.

[51] Thus, Figure 9a should be considered a theoretical high end-member scenario for methane plumes derived from airbursting bolide organics, and is certainly not representative of released methane expected from debris fields of more typical bolides impacting the surface or creating airbursts (sensu *Daubar et al.* [2010] or the 150-m bolide in section 3.3). More reasonable assumptions quickly reveal that large methane plumes from bolide airburst events are unlikely to create the 45 ppbv methane plume as reported by *Mumma et al.* [2009]. There are two major constraints on bolide airburst events that would decrease the methane plume concentrations significantly below 45 ppbv. First, the assumption that 100% of the organics is converted to methane over 120 sols is unlikely because the H/C of extraterrestrial organics (e.g., 0.70 for Murchison [*Naraoka et al.*, 2004]) implies a maximum conversion rate closer to 20% over long periods of time, not 100% over 120 sols. Second, the assumption that the total mass of the airbursting comet would be spread uniformly over the required area as a

30-nm thick planar sheet of debris is unlikely. Converting the 30 nm planar sheet to individual spherical particles (conversion factor of 1.9), a debris field composed of 57-nm spheres acting independently in the atmosphere and on the surface would yield the same methane flux rates as presented in Figure 9a. However, if the spherical particles were larger than 57 nm, the methane rate falls very quickly as the particle diameters increase.

[52] The decrease in methane abundance with larger particles is primarily caused by a reduction in the penetration of UV photons to internal layers of the larger particles [see *Moores and Schuerger*, 2012], and a decreased fraction of the Martian surface UV flux that actually strikes particles (Figure 6). Figure 9b depicts the effects of particle size on methane abundance in plumes. The scale bar on the right can be used to generate the methane flux for any assumed particle size by dividing a scale-bar value by the diameter of an assumed average particle distribution. For example, if the particle sizes are, on average, 100 nm, 1 μm, or 100 μm in diameter, the 150-m bolide scenario outlined in section 3.3 would yield only 19, 1.9, or 0.02 ppbv methane, respectively, to a plume matching the areal characteristics as reported by *Mumma et al.* [2009]. Only if all particle sizes are below 100 nm, fully exposed to solar UV, and assumed to be converted 100% to methane can the UV/CH4 process yield methane plumes that approach the 45 ppbv plumes reported by *Mumma et al.* [2009]. All three conditions seem very unlikely. Furthermore, many airbursts yield a wide range of debris particles and fragments, the largest of which are likely to impact the surface forming discrete crater clusters (Figure 8b). Based on the these limitations, we conclude that the UV/CH4 process is unlikely to yield large-scale methane plumes on Mars from dispersed airburst debris because a significant amount of each bolide mass will be composed of particles above 100 nm in diameter, and much of the cometary organics would not be immediately accessible to UV alteration on the Martian surface.

[53] And lastly, additional methane might be injected into the Martian atmosphere by smaller airbursts or direct impacts of 2–3 m diameter carbonaceous chondrites. Recent work on the rates of small bolide impacts or airbursts [*Daubar et al.*, 2010] suggests that at least 77 new impact events by 2–3 m diameter bolides are occurring on Mars each year (Eyr). Of these impacts, approximately 20% (i.e., 16 impacts) are likely to be carbonaceous chondrites, and at least half of these (i.e., 8 impacts) are likely to be airbursts [*Daubar et al.*, 2010]. Such a frequency of 2–3 m diameter carbonaceous chondrites, with a 10 wt% organic C content might inject an additional 0.23 pptv methane into the Martian atmosphere on an annual basis (Eyr). Balancing this impact rate of small carbonaceous chondrites and a 329 year methane destruction rate would yield an additional 0.076 ppbv methane accumulated over geological time. Higher carbon contents of impacting bolides (Figure 9a models up to 24 wt% C) would raise these values slightly.

4. Discussion

4.1. Average Global Methane Budget

[54] The UV/CH4 model is based on two widely accepted processes on Mars: the accretion of organics from IDPs and small carbonaceous chondrites [*Flynn*, 1996], and UV

photons between 190 and 400 nm reaching the surface [*Kuhn and Atreya*, 1979; *Cockell et al.*, 2000; *Moores et al.*, 2007; *Patel et al.*, 2003]. The current work was based on a study by *Stoker and Bullock* [1997] that demonstrated the production of methane from glycine exposed to a Mars-normal UV flux (200–400 nm) under Martian conditions at pressures between 50 and 100 mbar. Recently three studies have supported the plausibility of the UV/CH4 model operating on Mars by demonstrating the evolution of CH_3^- radicals [*Shkrob et al.*, 2010] and methane [*Keppler et al.*, 2012; *Schuerger et al.*, 2011] from UV irradiated organics under lab or simulated Martian conditions, respectively. The current work extends these studies and demonstrates the evolution of methane from the UV irradiation of authentic carbonaceous chondrite organics under Martian conditions at 6.9 mbar, and down to −80°C. The evolution of methane by the UV/CH4 process was found to be positively correlated to temperature (Figure 2), positively correlated to the concentration of organics present in the crushed and sieved chondrites (Figure 3), and decreased over time (Figure 4). Pressure may not affect the production of methane from UV-irradiated organics because methane evolution has been noted at 6.9 mbar [*Schuerger et al.*, 2011; current study], 50–100 mbar [*Stoker and Bullock*, 1997], and 1013 mbar [*Grätzel et al.*, 1989; *McLeod et al.*, 2008; *Shkrob et al.*, 2010; *Vigano et al.*, 2008]. In contrast, *Keppler et al.* [2012] suggest that low pressures near Martian conditions (10 mbar) boosted methane evolution compared to terrestrial pressures near 1013 mbar.

[55] And lastly, the production of methane from UV-irradiated Murchison organics was found to be *carbon-limited* on Mars (Figure 6), suggesting that all exposed organics can be degraded by UV photons over time. The global methane budget appears limited by the annual influx rate of the accreted organics and not by the UV flux. Although coevolved volatiles (e.g., CO_2, ethane, ethylene) have been reported with methane during the UV irradiation of organics [*Dey and Pushpa*, 2006; *Keppler et al.*, 2012; *McLeod et al.*, 2008; *Stoker and Bullock*, 1997], results from the current work, and related studies by *Schuerger et al.* [2011], failed to confirm the coevolution of other volatile organics (≤C_3 compounds) from the UV-irradiated chondrites down to 0.5 ppm. We chose a lower limit of 20% conversion as a 1st-order approximation for the C to CH4 pathway based on (1) the H/C ratio of 0.70 for Murchison [*Naraoka et al.*, 2004] suggests a CH4 evolution rate close to 18.9%, if H^+ is derived from IDP organics, and (2) additional H^+ ions may be supplied by other photochemistry processes in the atmosphere [*Krasnopolsky*, 2006; *Wong et al.*, 2003]. The selection of 20% conversion rate is consistent with a recent report on the UV irradiation of organics under Martian conditions that estimated a conversion rate of C to CH4 of between 8.5 and 55% [*Keppler et al.*, 2012].

[56] Based on model assumptions (section 2.4) and the data presented here, the UV/CH4 model predicts (i) a daily methane input of between 0.02 and 0.09 pptv per sol (for 20 and 100% conversion rates, respectively), (ii) an annual global input of 0.0064 and 0.033 ppbv] ppbv methane, and (iii) a globally averaged methane concentration between 2.2 and 11 ppbv accumulated over geological time. If the Lyman-α photolytic model for the long-term persistence (≥329 Eyr) of methane in the Martian atmosphere [*Lefèvre and Forget*,

2009] is the sole methane sink process on Mars, the UV/CH$_4$ model yields atmospheric concentrations of methane that are slightly lower or similar to current measurements of 10–15 ppbv by Earth-bound telescopes or the Planetary Fourier Spectrometer (PFS) on board Mars Express [*Fonti and Marzo*, 2010; *Formisano et al.*, 2004; *Geminale et al.*, 2008, 2011; *Krasnopolsky et al.*, 2004; *Mumma et al.*, 2009]. Assuming a methane lifetime of 329 years, the UV/CH$_4$ mechanism with accreted IDP organics could supply between 64 and 320 t of methane per year (i.e., for 20 and 100% conversion rates, respectively); similar to the modeled production rate of methane required to maintain 10 ppbv, as reported by *Atreya et al.* [2007] (126 t yr^{-1}; assuming a 600 yr CH$_4$ lifetime).

[57] Published reports for methane abundance in the Martian atmosphere have suggested that seasonal, latitudinal, and even diurnal changes are potentially being observed on Mars [*Fonti and Marzo*, 2010; *Formisano et al.*, 2004; *Geminale et al.*, 2008, 2011; *Krasnopolsky et al.*, 2004; *Mumma et al.*, 2009]. However, the UV/CH$_4$ model for IDP organics predicts very small-scale changes for daily and annual methane abundance on Mars, and fails to explain the ppbv seasonal, latitudinal, or diurnal changes because the daily and annual input of IDP organics to the Martian atmosphere are at least 3 orders of magnitude too small to generate the methane required to match published reports [*Moores and Schuerger*, 2012]. Seasonal, latitudinal, and diurnal changes may be occurring on Mars, but if present, are due to sink/source processes other than the UV/CH$_4$ mechanism.

4.2. UV/CH$_4$ Model for Methane Plumes

[58] The UV/CH$_4$ model for isotropically accreted IDP organics is unable to predict the size and abundance of methane found in recently reported plumes of 45 ppbv [*Mumma et al.*, 2009] or 50–60 ppbv [*Fonti and Marzo*, 2010]. In order for UV irradiation to degrade organics on Mars and yield the large methane signatures detected in the plumes (e.g., up to 19,000 t CH$_4$; *Mumma et al.* [2009]), very large amounts of organics must be emplaced or excavated on the surface all at once. Of the various impact scenarios tested to possibly explain methane plumes on Mars: (1) single large bolide impacts are rejected because they are inconsistent with the impact record of recent years, (2) single airburst events of coherent low-density bolides are rejected because such events do not appear capable of emplacing adequate carbon over the required area to permit the UV/CH$_4$ process to form plumes up to 45 ppbv, and (3) infrequent high-altitude airbursts of rubble-pile comets are rejected because the conversion rates of organics to methane must be unreasonably high, and the average particle diameters in the debris field must be unreasonably small to yield plumes up to 45 ppbv. Results from airburst modeling support the conclusion that a 150-m diameter low-density non-coherent rubble-pile comet can plausibly disperse adequate mass (up to 1.8×10^9 kg) over the required area (9×10^6 km^2) to match the spatial characteristics of the plumes as reported by *Mumma et al.* [2009]. Thus, the rejection of the airburst rubble-pile comet scenario is not due to airburst dynamics, but rather, it is due to the inability of the UV/CH$_4$ linked process to supply methane fast enough over 120 sols to have the methane detected as a discrete plume by Earth-bound telescopes or the PFS

instrument on board Mars Express [*Fonti and Marzo*, 2010; *Formisano et al.*, 2004; *Geminale et al.*, 2008, 2011; *Krasnopolsky et al.*, 2004; *Mumma et al.*, 2009].

[59] Methane plumes up to 60 ppbv have been reported on Mars [*Fonti and Marzo*, 2010; *Mumma et al.*, 2009]. The plumes appear for less than 1 Mars yr, and are scattered randomly around the surface. Such an episodic process argues strongly against stable and continuous subterranean sources like serpentinization [*Lyons et al.*, 2005; *Oze and Sharma*, 2005] or methanogenesis [*Max and Clifford*, 2000], but does argue in favor of a periodic process like the airburst scenario described here. *Mischna et al.* [2011] used the Mars Weather Research and Forecast (MarsWRF) General Circulation Model (GCM) model to suggest that it is very unlikely that the *Mumma et al.* [2009] plumes were the result of a point source emission because (1) the north/south extent of the 45 ppbv plumes requires a broad meridional source rather than a point emission, (2) the methane plume "…must have been derived from a near-instantaneous… event rather than a slow, steady emission…," and (3) that no known subsurface source process can match the temporally correlated release of methane over such a large distance. The Mars WRF modeling by *Mischna et al.* [2011] supports the hypothesis that airbursts of rubble-pile comets may be involved with methane plumes on Mars, but our modeling falls short in explaining how this process might work. Thus, although the preliminary airburst modeling reported here fails to fully explain the large methane plumes reported by *Fonti and Marzo* [2010] and *Mumma et al.* [2009], additional work might identify how impact-associated processes might trigger the near instantaneous release of methane over such wide areas.

4.3. Mixed UV/CH$_4$ Model for Global Methane on Mars

[60] We propose the following mixed UV/CH$_4$ linked model for methane abundance on Mars. We do not believe that seasonal, latitudinal, diurnal, and plume fluctuations can be easily explained by the UV/CH$_4$ model, and will be ignored for the current mixed UV/CH$_4$ model.

[61] First, the UV/CH$_4$ process appears capable of supplying a background global average of $\sim$2.2 ppbv methane for a 20% conversion rate from accreted IDPs with 10 wt% C (our study). Although two studies [*Keppler et al.*, 2012; *Stoker and Bullock*, 1997] reported coevolved species from UV irradiated organics under Martian conditions, the coevolved products (e.g., ethane, ethylene, propane) were generated at rates less than 1 order of magnitude lower than methane. Using the 20% conversion rate over time as reported here, a 600-year destruction rate for methane (high-end estimate of the Lyman-α UV destruction process [*Lefèvre and Forget*, 2009]), and 12 wt% for IDPs [*Thomas et al.*, 1993], the theoretical maximum global average for methane would be $\sim$4.8 ppbv. Assuming no other source/sink processes, we conclude that between 2.2 and 4.8 ppbv methane are likely created on Mars by the UV destruction of accreted IDP organics.

[62] Second, approximately 8 impacts and 8 airbursts of small carbonaceous bolides ($\sim$2–3 m in diameter) appear to be falling on Mars each year [*Daubar et al.*, 2010]. From these carbonaceous bolides (assuming 10 wt% C), we estimate that an additional 0.23 pptv methane might be injected

into the Martian atmosphere on an annual basis (Eyr). Balancing this impact rate of small carbonaceous chondrites and a 329 year methane destruction rate would yield an additional 0.076 ppbv methane accumulated over geological time. If the methane destruction rate was closer to the upper bound of 600 years [*Lefèvre and Forget*, 2009], as much as 0.138 ppbv might be added to the global methane budget from small impacts and airbursts of bolides ≤2–3 m in diameter.

[63] Third, airburst modeling suggests that for entry angles of 45°, 60°, or 80°, the maximum sizes of bolides that would create airbursts in the Martian atmosphere would be 93, 131, or 378 m, respectively. Assuming that all debris is scattered from the range of bolides listed above, and no impact craters are formed, then airbursting bolides might still add significant extraterrestrial C into the Martian system. Although the modeling in section 3.4 appears unable to explain large methane plumes from airbursts, any surviving C from airbursts would be dispersed onto the Martian terrain, and would presumably supply organics to the UV/CH₄ process over time. The current study has not modeled the C inputs to Mars by airbursting bolides between 3 and 378 m in diameter, but it is plausible that significant levels of organics can be added to the Martian surface over geological time. Furthermore, *Moores and Schuerger* [2012] describe several mechanisms on Mars that would act to mechanically and chemically disaggregate the landed debris from airbursts, rendering new UV reactive sights over time. Thus, even low-frequency medium-sized airbursts of low density bolides might increase the global budget of methane over time, even if such airbursts fail to create observable methane plumes. The difficulty in modeling airbursts in planetary atmospheres is that the airbursts can often leave no significant evidence of their occurrence. However, small periodic spikes in atmospheric methane detected by the Mars Science Laboratory (MSL) rover or a Trace Gas Orbiter (TGO) like spacecraft may give evidence of both the size and frequency of airbursts by carbonaceous bolides.

4.4. MSL and TGO Predictions

[64] Results from the current study are used to make five predictions relevant to methane detection for the upcoming MSL rover or TGO orbiter missions. (1) If the conversion of C to CH₄ is confirmed to be approximately 20% efficient, the UV/CH₄ model predicts a globally averaged abundance of ~2.2 to 4.8 ppbv methane, a level that should be easily measured by the MSL rover and TGO orbiter. (2) The MSL rover has a minimum detection limit of ~1 pptv [*Webster and Mahaffy*, 2011], and a TGO-like orbiter is expected to have a low detection limit of ~3 pptv [*Cloutis et al.*, 2011; *Wennberg et al.*, 2011] to 10 pptv [*Zurek et al.*, 2010]. Thus, both the MSL and a TGO-like mission will be able to confirm the C to CH₄ conversion rate by the UV/CH₄ alteration of IDP organics as long as the conversion rate is greater than 0.01% for MSL or 0.03% for TGO. (3) Any spikes above the measured methane background level will give insights into the size and frequency of small airbursts of carbonaceous bolides occurring upwind of the MSL landing site. (4) The TGO orbiter should be able to see airbursts as small methane spikes above the background as long as the hot spots (i.e., plumes) are above ~10 pptv, and the areal extent of the small methane plumes are greater than the spatial resolution

of the Mars Atmospheric Trace Molecule Occultation Spectrometer (MATMOS) instrument [*Wennberg et al.*, 2011]. For example, the model in Figure 9b suggests that small airbursts with particles ranging in size between 1 and 30 μm might yield small short-lived plumes between 1 ppbv to 10 pptv, respectively. (5) Based on new modeling presented here and elsewhere [*Moores and Schuerger*, 2012], the MSL rover is unlikely to see diurnal changes in methane abundance in the atmosphere caused by the UV/CH₄ process because the average daily rate for new methane through the process is only 0.09 pptv per sol, well below the Sample Analysis on Mars/Tunable Laser Spectrometer (SAM/TLS) detection limits of ~1 pptv on MSL. Thus, an earlier prediction by *Schuerger et al.* [2011] on the possibility of MSL detecting diurnal changes in methane abundance on Mars must be retracted.

5. Conclusions

[65] The primary finding of the current study is that methane is a by-product of the UV irradiation of authentic carbonaceous chondritic materials under Martian conditions. Results are consistent with earlier work [*Keppler et al.*, 2012; *Schuerger et al.*, 2011; *Shkrob et al.*, 2010; *Stoker and Bullock*, 1997], and confirm that a UV/CH₄ linked mechanism is likely operating on Mars for accreted organics. A 20% conversion rate for C to CH₄ modeled here would yield a global average of ~2.2 ppbv over geologic time. However, assuming a 20% conversion rate of C to CH₄, a 600 year methane destruction rate, and 12 wt% for IDPs, the global average for methane might approach ~4.8 ppbv from the UV/CH₄ process. Global background levels of methane above 4.8 ppbv would imply that significant amounts of accreted organics (e.g., airbursts of rubble-pile comets) are arriving on Mars, or the conversion rate is greater than 20%.

[66] Direct surface impacts, airbursts of coherent bolides, and cascading airbursts of low-density non-coherent rubble-pile comets were rejected as plausible sources of large methane plumes on Mars due to unrealistic assumptions required to convert the dispersed organics into methane by the UV/CH₄ process. But smaller plumes in both size and areal extent might be detectable on future missions. And lastly, the UV/CH₄ mechanism cannot easily explain spatial and temporal heterogeneity of methane in the Martian atmosphere. If the seasonal, latitudinal, and diurnal methane observations are confirmed on Mars, they must be created by source/sink processes other than the UV/CH₄ mechanism.

[67] The UV/CH₄ model predicts a range of methane abundance in the Martian atmosphere between 2.2 and 11 ppbv, depending on model assumptions, that is consistent with the reported levels of methane on Mars [*Fonti and Marzo*, 2010; *Formisano et al.*, 2004; *Geminale et al.*, 2008, 2011; *Krasnopolsky et al.*, 2004; *Mumma et al.*, 2009]. Thus, the UV/CH₄ model can explain some of the globally averaged methane budget on Mars without invoking subsurface processes like serpentinization or methanogenesis. And lastly, the MSL and TGO missions will be able to verify and constrain specific assumptions of the UV/CH₄ model.

[68] There are two key research gaps that must be studied in order to refine the UV/CH₄ model for Mars. First, what is the precise mass balance of methane to all other coevolved

volatile species by the UV irradiation of organics under Martian conditions? We selected a 20% conversion rate for the UV/CH_4 process to change C to CH_4 based on four criteria (see Assumption 5, section 2.4). However, more precise experiments are required to fully characterize the C to CH_4 conversion rate by UV irradiation of organics on Mars. In particular, the effects of UV-only versus oxidant-only degradation processes must be studied to determine if methane is the dominant constituent of the volatiles given off by the UV irradiation of organics on Mars. Based on the work of *Keppler et al.* [2012] and *Stoker and Bullock* [1997] it appears that methane is produced at a rate that is over 1 order of magnitude higher than the coevolved species ethane, ethylene, propane, and propylene. Based on their work, we may be able to constrain organic volatiles to a 90:10 ratio of methane to other species. Oxidants have been shown to be created by the UV irradiation of Mars analog soils [*Yen et al.*, 2000], oxidants can form on mineral surfaces [*Davila et al.*, 2008], oxidants appear capable of degrading organics under conditions relevant for Mars [*McDonald et al.*, 1998; *Oró and Holzer*, 1979], and CO_2 has been shown to be a by-product of oxidant degradation of organics [*Tsapin et al.*, 2000]. However, what is currently unknown is whether C is lost to CO_2 (or CO) by the UV irradiation of organics under Martian conditions by either UV-only, oxidant-only, or mixed reactions; and whether the rate of CO_2 evolution from oxidant-only reactions exceed the rate of methane evolution by the UV/CH_4 process [*Keppler et al.*, 2012; *Schuerger et al.*, 2011; *Stoker and Bullock*, 1997; current study].

[69] And second, does methane evolution from UV irradiated organics continue until all organics are destroyed, or does the UV-degradation of organics on Mars attenuate over time leaving some mass of C present as refractory molecules? *Archer et al.* [2010] report that UV irradiation of mellitic acid, trimellitic acid, and sodium benzoate did not completely destroy all organic molecules in the samples, and suggested that a rime of UV-absorbing refractory molecules might be protecting unaltered organics in deeper layers. In the current study, methane evolution from UV irradiation of Murchison organics decreased over 20 days in the Mars chamber simulating 120 sols on Mars (Figure 4). In both cases, the complete destruction of the UV-exposed organics was not demonstrated. Thus, long-term experiments must be undertaken with IDP or Murchison-like organics exposed to Mars-relevant UV and environmental conditions in order to accurately constrain the attenuation of the methane generation process over time. However, care must be taken to also include periodic mixing and crushing of the UV irradiated organics in order to simulate the mechanical degradation of IDPs likely occurring on Mars [*Moores and Schuerger*, 2012]. Even if a rime of UV refractory organic forms on IDPs [sensu *Archer et al.*, 2010], mechanical shearing might eventually expose fresh surfaces that would continue the degradation process [*Moores and Schuerger*, 2012].

References

Archer, P. D., Jr., H. Imanaka, M. A. Smith, W. V. Boynton, and P. H. Smith (2010), Pyrolysis of UV-irradiated organic molecules: Investigating potential Martian organics, *LPI Contrib.*, *1538*, 5600.

Artemieva, N. A., and V. V. Shuvalov (2001), Motion of a fragmented meteoroid through the planetary atmosphere, *J. Geophys. Res.*, *106*(E2), 3297–3309, doi:10.1029/2000JE001264.

Atreya, S. K., P. R. Mahaffy, and A.-S. Wong (2007), Methane and related species on Mars: Origin, loss, implications for life and habitability, *Planet. Space Sci.*, *55*, 358–369, doi:10.1016/j.pss.2006.02.005.

Barlow, N. G. (2005), A review of Martian impact crater ejecta structures and their implications for target properties, in *Large Meteorite Impacts III*, edited by T. Kenkmann et al., *Spec. Pap. Geol. Soc. Am.*, *384*, 433–442.

Biemann, K., and J. M. Lavoi Jr. (1979), Some final conclusions and supporting experiments related to the search for organic compounds on the surface of Mars, *J. Geophys. Res.*, *84*(B14), 8385–8390, doi:10.1029/JB084iB14p08385.

Bland, P. A., and T. S. Smith (2000), Meteorite accumulation on Mars, *Icarus*, *144*, 21–26, doi:10.1006/icar.1999.6253.

Botta, O., and J. L. Bada (2002), Extraterrestrial organic compounds in meteorites, *Surv. Geophys.*, *23*, 411–467, doi:10.1023/A:1020139302770.

Chyba, C., and C. Sagan (1992), Endogenous production, exogenous delivery and impact-shock synthesis of organic molecules: An inventory for the origins of life, *Nature*, *355*, 125–132, doi:10.1038/355125a0.

Cloutis, E. A., et al. (2011), ExoMars Trace Gas Orbiter MATMOS Instrument: Preliminary strategy for development of a dust spectral library, *Proc. Lunar Planet. Sci. Conf.*, *42*, Abstract 1175.

Cockell, C. S., D. C. Catling, W. L. Davis, K. Snook, R. L. Kepner, P. Lee, and C. P. McKay (2000), The ultraviolet environment of Mars: Biological implications past, present, and future, *Icarus*, *146*, 343–359, doi:10.1006/icar.2000.6393.

Daubar, I. J., A. S. McEwen, S. Byrne, C. M. Dundas, M. Kennedy, and B. A. Ivanov (2010), The current Martian cratering rate, *LPI Contrib.*, *1533*, 1978.

Davila, A. F., A. G. Fairen, L. Gago-Duport, C. R. Stoker, R. Amils, R. Bonaccorsi, J. Zavaleta, D. Lim, D. Schulze-Makuch, and C. P. McKay (2008), Subsurface formation of oxidants on Mars and implications for the preservation of organic biosignatures, *Earth Planet. Sci. Lett.*, *272*, 456–463, doi:10.1016/j.epsl.2008.05.015.

Desai, P. N., J. T. Schofield, and M. E. Lisano (2005), Flight reconstruction of the Mars Pathfinder disk-gap-band parachute drag coefficients, *J. Spacecr. Rockets*, *42*, 672–676, doi:10.2514/1.5996.

Dey, G. R., and K. K. Pushpa (2006), Methane generated during phtotocatalytic redox reaction of alcohols on TiO_2 suspension in aqueous solutions, *Res. Chem. Intermediates*, *32*, 725–736, doi:10.1163/156856706778606462.

Ehrenfreund, P., M. P. Bernstein, J. P. Dworkin, S. A. Sandford, and L. J. Allamandola (2001), The photostability of amino acids in space, *Astrophys. J.*, *550*, L95–L99, doi:10.1086/319491.

Flynn, G. J. (1996), The delivery of organic matter from asteroids and comets to the early surface of Mars, *Earth Moon Planets*, *72*, 469–474, doi:10.1007/BF00117551.

Flynn, G. J., and D. S. McKay (1990), An assessment of the meteoritic contribution to the Martian soil, *J. Geophys. Res.*, *95*(B9), 14,497–14,509, doi:10.1029/JB095iB09p14497.

Flynn, G. J., L. P. Keller, M. Feser, S. Wirick, and C. Jacobsen (2003), The origin of organic matter in the solar system: Evidence from the interplanetary dust particles, *Geochim. Cosmochim. Acta*, *67*(24), 4791–4806, doi:10.1016/j.gca.2003.09.001.

Flynn, G. J., S. Wirick, L. P. Keller, C. Jacobsen, and S. A. Sandford (2010), Organic coatings on individual grains in CP IDPs: Implications for the formation mechanism of pre-biotic organic matter and for grain sticking in the early solar system, *LPI Contrib.*, *1533*, 1079.

Fonti, S., and G. A. Marzo (2010), Mapping the methane on Mars, *Astron. Astrophys.*, *512*, A51, doi:10.1051/0004-6361/200913178.

Formisano, V., S. Atreya, T. Encrenaz, N. Ignatiev, and M. Giuranna (2004), Detection of methane in the atmosphere of Mars, *Science*, *306*, 1758–1761, doi:10.1126/science.1101732.

Garry, J. R. C., I. L. ten Kate, Z. Martins, P. Nornberg, and P. Ehrenfreund (2006), Analysis and survival of amino acids in Martian regolith analogs, *Meteorit. Planet. Sci.*, *41*, 391–405, doi:10.1111/j.1945-5100.2006.tb00470.x.

Geminale, A., V. Formisano, and M. Giuranna (2008), Methane in Martian atmosphere: Average spatial, diurnal, and seasonal behavior, *Planet. Space Sci.*, *56*, 1194–1203, doi:10.1016/j.pss.2008.03.004.

Geminale, A., V. Formisano, and G. Sindoni (2011), Mapping methane in Martian atmosphere with PFS-MEX data, *Planet. Space Sci.*, *59*, 137–148, doi:10.1016/j.pss.2010.07.011.

Golombek, M. P., et al. (1997), Overview of the Mars Pathfinder mission and assessment of landing site predictions, *Science*, *278*, 1743–1748, doi:10.1126/science.278.5344.1743.

Grätzel, M., K. R. Thampi, and J. Kiwi (1989), Methane oxidation at room temperature and atmospheric pressure activated by light via polytungstate dispersed on titania, *J. Phys. Chem.*, *93*, 4128–4132, doi:10.1021/j100347a050.

Haberle, R. M., et al. (2001), On the possibility of liquid water on present-day Mars, *J. Geophys. Res.*, *106*, 23,317–23,326, doi:10.1029/2000JE001360.

Herrick, R. R., and K. K. Hessen (2006), The planforms of low-angle impact craters in the northern hemisphere of Mars, *Meteorit. Planet. Sci.*, *41*, 1483–1495, doi:10.1111/j.1945-5100.2006.tb00431.x.

Jeong, I.-S., J. H. Kim, and S. Im (2003), Ultraviolet-enhanced photodiode employing *n*-ZnO/*p*-Si structure, *Appl. Phys. Lett.*, *83*, 2946–2948, doi:10.1063/1.1616663.

Johnson, J. R., W. M. Grundy, and M. T. Lemmon (2003), Dust deposition at the Mars Pathfinder landing site: Observations and modeling of visible/near infrared spectra, *Icarus*, *163*, 330–346, doi:10.1016/S0019-1035(03)00084-8.

Keppler, F., J. T. G. Hamilton, M. Braß, and T. Rockmann (2006), Methane emissions from terrestrial plants under aerobic conditions, *Nature*, *439*, 187–191, doi:10.1038/nature04420.

Keppler, F., I. Vigano, A. McLeod, U. Ott, M. Früchtl, and T. Röckmann (2012), Ultraviolet-radiation-induced methane emissions from meteorites and the Martian atmosphere, *Nature*, *486*, 93–96, doi:10.1038/nature11203.

Kieffer, H. H. (1976), Soil and surface temperatures at the Viking landing sites, *Science*, *194*, 1344–1346, doi:10.1126/science.194.4271.1344.

Krasnopolsky, V. A. (2006), Photochemistry of the Martian atmosphere: Seasonal, latitudinal, and diurnal variations, *Icarus*, *185*, 153–170, doi:10.1016/j.icarus.2006.06.003.

Krasnopolsky, V. A., J. P. Maillard, and T. C. Owen (2004), Detection of methane in the Martian atmosphere: Evidence for life?, *Icarus*, *172*, 537–547, doi:10.1016/j.icarus.2004.07.004.

Kuhn, W. R., and S. K. Atreya (1979), Solar radiation incident on the Martian surface, *J. Mol. Evol.*, *14*, 57–64, doi:10.1007/BF01732367.

Lefèvre, F., and F. Forget (2009), Observed variations of methane on Mars unexplained by known atmospheric chemistry and physics, *Nature*, *460*, 720–723, doi:10.1038/nature08228.

Lefèvre, F., S. Lebonnois, F. Montmessin, and F. Forget (2004), Three-dimensional modeling of ozone on Mars, *J. Geophys. Res.*, *109*, E07004, doi:10.1029/2004JE002268.

Lemmon, M. T., et al. (2004), Atmospheric imaging results from the Mars Exploration Rovers: Spirit and Opportunity, *Science*, *306*, 1753–1756, doi:10.1126/science.1104474.

Lyons, J. R., C. Manning, and F. Nimmo (2005), Formation of methane on Mars by fluid-rock interaction in the crust, *Geophys. Res. Lett.*, *32*, L13201, doi:10.1029/2004GL022161.

Malin, M. C., K. S. Edgett, L. V. Posiolova, S. M. McColley, and E. Z. Noe Dobrea (2006), Present-day impact cratering rate and contemporary gully activity on Mars, *Science*, *314*, 1573–1577, doi:10.1126/science.1135156.

Max, M. D., and S. M. Clifford (2000), The state, potential distribution, and biological implications of methane in the Martian crust, *J. Geophys. Res.*, *105*(E2), 4165–4171, doi:10.1029/1999JE001119.

McDonald, G. D., E. de Vanassay, and J. R. Buckley (1998), Oxidation of organic macromolecules by hydrogen peroxide: Implications for stability of biomarkers on Mars, *Icarus*, *132*, 170–175, doi:10.1006/icar.1998.5896.

McLeod, A. R., S. C. Fry, G. J. Loake, D. J. Messenger, D. S. Reay, K. A. Smith, and B.-W. Yun (2008), Ultraviolet radiation drives methane emissions from terrestrial plant pectins, *New Phytol.*, *180*, 124–132, doi:10.1111/j.1469-8137.2008.02571.x.

Melosh, H. J. (1989), *Impact Cratering: A Geologic Process*, 245 pp., Oxford Univ. Press, New York.

Mischna, M. A., M. Allen, M. I. Richardson, C. E. Newman, and A. D. Toigo (2011), Atmospheric modeling of Mars methane surface releases, *Planet. Space Sci.*, *59*, 227–237, doi:10.1016/j.pss.2010.07.005.

Moores, J. E., and A. C. Schuerger (2012), A meteoritic origin for the putative surface reservoir of organic carbon on Mars and relevance to the detection of methane in the Martian atmosphere, *J. Geophys. Res.*, doi:10.1029/2012JE004060, in press.

Moores, J. E., P. H. Smith, R. Tanner, A. C. Schuerger, and K. Venkateswaran (2007), The shielding effect of small-scale Martian surface geometry on ultraviolet flux, *Icarus*, *192*, 417–433, doi:10.1016/j.icarus.2007.07.003.

Moores, J. E., J. D. Pelletier, and P. H. Smith (2008), Crack propagation by differential insolation on desert surface clasts, *Geomorphology*, *102*, 472–481, doi:10.1016/j.geomorph.2008.05.012.

Mumma, M. J., G. L. Villanueva, R. E. Novak, T. Hewgama, B. P. Bonev, M. A. DiSanti, A. M. Mandell, and M. D. Smith (2009), Strong release of

methane on Mars in northern summer 2003, *Science*, *323*(5917), 1041–1045, doi:10.1126/science.1165243.

Naraoka, H., H. Mita, M. Komiya, S. Yoneda, H. Kojima, and A. Shimoyama (2004), A chemical sequence of macromolecular organic matter in the CM chondrites, *Meteorit. Planet. Sci.*, *39*, 401–406, doi:10.1111/j.1945-5100.2004.tb00101.x.

Navarro-González, R., E. Vargas, J. de la Rosa, A. C. Raga, and C. P. McKay (2010), Reanalysis of the Viking results suggests perchlorate and organics at mid-latitudes on Mars, *J. Geophys. Res.*, *115*, E12010, doi:10.1029/2010JE003599.

Oró, J., and G. Holzer (1979), The photolytic degradation and oxidation of organic compounds under simulated Martian conditions, *J. Mol. Evol.*, *14*, 153–160, doi:10.1007/BF01732374.

Owen, T. (1992), The composition and early history of the atmosphere of Mars, in *Mars*, edited by H. H. Kieffer et al., pp. 818–834, Univ. of Ariz. Press, Tucson.

Oze, C., and M. Sharma (2005), Have olivine, will gas: Serpentinization and the abiogenic production of methane on Mars, *Geophys. Res. Lett.*, *32*, L10203, doi:10.1029/2005GL022691.

Patel, M. R., A. Bérces, C. Kolb, H. Lammer, P. Rettberg, J. C. Zarnecki, and F. Selsis (2003), Seasonal and diurnal variations in Martian surface ultraviolet irradiation: Biological and chemical implications for the Martian regolith, *Int. J. Astrobiol.*, *2*, 21–34, doi:10.1017/S1473550402001180.

Perrier, S., et al. (2006), Global distribution of total ozone on Mars from SPICAM/MEX UV measurements, *J. Geophys. Res.*, *111*, E09S06, doi:10.1029/2006JE002681.

Popova, O., I. Nemtchinov, and W. K. Hartmann (2003), Bolides in the present and past Martian atmosphere and effects on cratering processes, *Meteorit. Planet. Sci.*, *38*, 905–925, doi:10.1111/j.1945-5100.2003.tb00287.x.

Preblich, B. S., A. S. McEwen, and D. M. Studer (2007), Mapping rays and secondary craters from the Martian crater Zunil, *J. Geophys. Res.*, *112*, E05006, doi:10.1029/2006JE002817.

Quay, P., J. Stutsman, D. Wilbur, A. Snover, E. Dlugokencky, and T. Brown (1999), The isotopic composition of atmospheric methane, *Global Biogeochem. Cycles*, *13*, 445–461, doi:10.1029/1998GB900006.

Schramm, L. S., D. E. Bronwlee, and M. M. Wheelock (1989), Major element composition of stratospheric micrometeorites, *Meteoritics*, *24*, 99–112, doi:10.1111/j.1945-5100.1989.tb00950.x.

Schuerger, A. C., R. L. Mancinelli, R. G. Kern, L. J. Rothschild, C. P. Mc, and C. P. Kay (2003), Survival of endospores of *Bacillus subtilis* on spacecraft surfaces under simulated Martian environments: Implications for the forward contamination of Mars, *Icarus*, *165*, 253–276, doi:10.1016/S0019-1035(03)00200-8.

Schuerger, A. C., J. T. Richards, P. E. Hintze, and R. Kern (2005), Surface characteristics of spacecraft components affect the aggregation of microorganisms and may lead to different survival rates of bacteria on Mars landers, *Astrobiology*, *5*, 545–559, doi:10.1089/ast.2005.5.545.

Schuerger, A. C., J. T. Richards, D. A. Newcombe, and K. Venkateswaran (2006), Rapid inactivation of seven *Bacillus* spp. under simulated Mars UV irradiation suggests minimum forward contamination around landing sites, *Icarus*, *181*, 52–62, doi:10.1016/j.icarus.2005.10.008.

Schuerger, A. C., P. Fajardo-Cavazos, C. A. Clausen, J. E. Moores, P. H. Smith, and W. L. Nicholson (2008), Slow degradation of ATP in simulated Martian environments suggests long residence times for the biosignature molecule on spacecraft surfaces, *Icarus*, *194*, 86–100, doi:10.1016/j.icarus.2007.10.010.

Schuerger, A. C., C. Clausen, and D. Britt (2011), Methane evolution from UV-irradiated spacecraft materials under simulated Martian conditions: Implications for the Mars Science Laboratory (MSL) mission, *Icarus*, *213*, 393–403, doi:10.1016/j.icarus.2011.02.017.

Shkrob, I. A., S. D. Chemerisov, and T. W. Marin (2010), Photocatalytic decomposition of carboxylated molecules on light-exposed Martian regolith and its relation to methane production on Mars, *Astrobiology*, *10*, 425–436, doi:10.1089/ast.2009.0433.

Spanovich, N., et al. (2006), Surface and near-surface atmospheric temperatures for the Mars Exploration Rover landing sites, *Icarus*, *180*, 314–320, doi:10.1016/j.icarus.2005.09.014.

Steel, D. (1998), Distributions and moments of asteroid and comet impact speeds upon Earth and Mars, *Planet. Space Sci.*, *46*, 473–478, doi:10.1016/S0032-0633(97)00232-8.

Stoker, C. R., and M. A. Bullock (1997), Organic degradation under simulated Martian conditions, *J. Geophys. Res.*, *102*(E5), 10,881–10,888, doi:10.1029/97JE00667.

Summers, M. E., B. J. Lieb, E. Chapman, and Y. L. Yung (2002), Atmospheric biomarkers of subsurface life on Mars, *Geophys. Res. Lett.*, *29*(24), 2171, doi:10.1029/2002GL015377.

Svetsov, V. V., I. V. Nemtchinov, and A. V. Teterev (1995), Disintegration of large meteoroids in Earth's atmosphere: Theoretical models, *Icarus*, *116*, 131–153, doi:10.1006/icar.1995.1116.

ten Kate, I. L., J. R. C. Garry, Z. Peeters, B. Foing, and P. Ehrenfreund (2006), The effects of Martian near surface conditions on the photochemistry of amino acids, *Planet. Space Sci.*, *54*, 296–302, doi:10.1016/j.pss.2005.12.002.

Thomas, K. L., G. E. Blanford, L. P. Keller, W. Klöck, and D. S. McKay (1993), Carbon abundance and silicate mineralogy of anhydrous interplanetary dust particles, *Geochim. Cosmochim. Acta*, *57*, 1551–1566, doi:10.1016/0016-7037(93)90012-L.

Tomasko, M. G., L. R. Doose, M. T. Lemmon, P. H. Smith, and E. Wegryn (1999), Properties of dust in the Martian atmosphere from the imager for Mars Pathfinder, *J. Geophys. Res.*, *104*(E4), 8987–9007, doi:10.1029/1998JE900016.

Tomasko, M. G., et al. (2005), Rain, winds and haze during the Huygens probe's descent to Titan's surface, *Nature*, *438*(7069), 765–778, doi:10.1038/nature04126.

Tornabene, L. L., et al. (2006), Identification of large (2–10 km) rayed craters on Mars in THEMIS thermal infrared images: Implications for possible Martian meteorite source regions, *J. Geophys. Res.*, *111*, E10006, doi:10.1029/2005JE002600.

Tsapin, A. I., M. G. Goldfeld, G. D. McDonald, and K. H. Nealson (2000), Iron(VI): Hypothetical candidate for the Martian oxidant, *Icarus*, *147*, 68–78, doi:10.1006/icar.2000.6437.

Vigano, I., H. van Weeldon, R. Holzinger, F. Keppler, and T. Rockman (2008), Effect of UV radiation and temperature on the emission of methane from plant biomass and structural components, *Biogeosci. Discuss.*, *5*, 243–270, doi:10.5194/bgd-5-243-2008.

Webster, C. R., and P. R. Mahaffy (2011), Determining the local abundance of Martian methane and its' ¹³C/¹²C and D/H isotopic ratios for comparison with related gas and soil analysis on the 2011 Mars Science Laboratory (MSL) mission, *Planet. Space Sci.*, *59*(2–3), 271–283, doi:10.1016/j.pss.2010.08.021.

Wennberg, P. O., et al. (2011), MATMOS: The Mars Atmospheric Trace Molecule Occultation Spectrometer, paper presented at Fourth International Workshop on the Mars Atmosphere: Modelling and Observations, Lab. de Meteorol. Dyn., Paris, 8–11 Feb.

Wong, A.-S., S. K. Atreya, and T. Encrenaz (2003), Chemical markers of possible hotspots on Mars, *J. Geophys. Res.*, *108*(E4), 5026, doi:10.1029/2002JE002003.

Yen, A. S., S. S. Kim, M. H. Hecht, M. S. Frant, and B. Murray (2000), Evidence that the reactivity of the Martian soil is due to superoxide ions, *Science*, *289*, 1909–1912, doi:10.1126/science.289.5486.1909.

Zahnle, K. J. (1992), Airburst origin of dark shadows on Venus, *J. Geophys. Res.*, *97*(E6), 10,243–10,255, doi:10.1029/92JE00787.

Zent, A. P., and C. P. McKay (1994), The chemical reactivity of the Martian soil and implications for future missions, *Icarus*, *108*, 146–157, doi:10.1006/icar.1994.1047.

Zurek, R. W., A. Chicarro, M. A. Allen, J.-L. Bertaux, R. T. Clancy, F. Daerdenm, V. Formisano, J. B. Garvin, G. Neukum, and M. D. Smith (2010), Assessment of a 2016 mission concept: The search for trace gasses in the atmosphere of Mars, *Planet. Space Sci.*, *59*(2–3), 284–291, doi:10.1016/j.pss.2010.07.007.